AN ABSTRACT OF THE THESIS OF

David Burl Ellis (Name) for the Master of Science (Degree)

in OCEANOGRAPHY (Major) presented on April 14, 1972 (Date)

Title: HOLOCENE SEDIMENTS OF THE SOUTH ATLANTIC OCEAN: THE CALCITE COMPENSATION DEPTH AND CONCENTRATIONS OF CALCITE, OPAL AND QUARTZ

Abstract approved: Redacted for privacy

Ted C. Moore, Jr.

The concentrations of calcite, opal and quartz have been measured in 113 South Atlantic core tops. The remainder of the total sample has been calculated as clay. A method for the quantitative determination of opal has been developed.

Calcite is the dominant factor in South Atlantic sediments; its pattern can be explained by bottom water circulation. Opal is primarily found in two bands - near the Equator and around 50° S. The distribution of opal resembles that of surface productivity. Quartz occurs near coastlines but also contains a significant ice-rafted component south of 35° S. Clay, probably consisting of kaolinite and illite, is principally found in the western Brazil Basin and extending southward into the Angola Basin from the Congo River mouth.

The calcite compensation level is not meaningfully determined

for the South Atlantic as a whole; it is necessary to divide data into basins. The levels obtained are: Brazil and northern Argentine Basins - 4800 m, Cape Basin - 5100 m, Angola Basin - 5400 m or deeper. Physico-chemical factors are more important than biological ones in determining the calcite compensation level.

Holocene Sediments of the South Atlantic Ocean: The Calcite Compensation Depth and Concentrations of Calcite, Opal and Quartz

by

David Burl Ellis

A THESIS

submitted to

Oregon State University

in partial fulfillment of
the requirements for the
degree of

Master of Science

June 1972

APPROVED:

Redacted for privacy

Assistant Professor of Oceanography
in charge of major

Redacted for privacy

Chairman of Department of Oceanography

Redacted for privacy

Dean of Graduate School

Date thesis is presented April 14, 1972

Typed by Marjorie Hay for David Burl Ellis

ACKNOWLEDGEMENTS

I would like to thank Dr. T. C. Moore for his guidance as my major professor and Drs. Tj. H. van Andel and G. Ross Heath for their aid and advice on all phases of this work. Dr. Richard W. Couch served on my committee as my minor professor. I was helped greatly in core sampling at Scripps Institution of Oceanography by William R. Riedel, Phyllis B. Helms, and Thomas C. Walsh. Sampling of Lamont-Doherty Geological Observatory cores was made possible by Dr. James D. Hays, Roy R. Capo and Dorothy S. Ultsch. The Lamont cores were obtained on the following grants: ONR (N0014-67-A-0108-0004) and NSF - GA - 29460 B. Dr. Karl K. Turekian of Yale University generously supplied data through the intermediary of Dr. E. Julius Dasch. The investigation was supported by grant GA-15316 of the National Science Foundation to Dr. Tj. H. van Andel.

TABLE OF CONTENTS

LIST OF FIGURES

LIST OF TABLES

HOLOCENE SEDIMENTS OF THE SOUTH ATLANTIC OCEAN: THE CALCITE COMPENSATION DEPTH AND CONCENTRATIONS OF CALCITE, OPAL AND QUARTZ

INTRODUCTION

The South Atlantic Ocean is one of the best studied of the world's oceans. This fact makes the area an ideal site for detailed quantitative studies of sediments, since adequate knowledge about the oceanographic processes responsible for the sediment distribution and type can be applied to the problem. In addition, a large number of deep-sea cores is available.

The sediment pattern of the South Atlantic has been known in a general way since the Challenger expedition report (Murray and Renard, 1891). Murray and Renard found red clay in the deep basins, calcium carbonate oozes on the ridges, terrigenous deposits close to land, and diatom ooze in the far south (around 50° S). This picture has not been substantially changed since their report.

The Meteor expedition of 1925-1927 accumulated the greatest amount of information about the South Atlantic of any single project. Pratje (1939) refined and explained the pattern of Murray and Renard (1891) by applying the physical oceanographic data of Wüst (1936), and considered the flow of the Antarctic Bottom Water (AABW) to be the single most important factor responsible for the sediment

distribution. The AABW flows northward from Antarctica along the bottom of the Argentine Basin through breaches in the Rio Grande Rise and into the Brazil Basin to the west of the Mid-Atlantic Ridge. To the east of the ridge it flows from the Atlantic-Antarctic Basin through the Agulhas Basin into the Cape Basin. However, the Walvis Ridge presents a barrier which, in conjunction with the Mid-Atlantic Ridge, prohibits influx of AABW to the Angola Basin except through the Romanche Fracture Zone at the Equator. Since the cold AABW aids in the dissolution of calcium carbonate, the flow pattern accounts for the presence of calcareous oozes in the Angola Basin while they are absent in the other three basins.

This theory has been adhered to up to the present time. However, little quantitative work has been done. Turekian (1964) has published a map of the $CaCO_3$ concentrations in Atlantic Ocean sediments, which however, extends only to 40° South and contains only broad subdivisions. Most of the quantitative work has been devoted to clay mineralogy, e.g., Biscaye (1965) and Goldberg and Griffin (1964). Biscaye (1965) also shows quartz concentrations indirectly in the form of a map of quartz to illite ratios. Lisitzin (1971) has published a worldwide map of biogenic silica (opal) concentrations.

There is, in the world oceans, a large difference in $CaCO_3$ concentration between ridges and deep basins. A plot of sediment $CaCO_3$ content versus water depth, for example in the Equatorial

Pacific, shows that most of the change in $CaCO_3$ percentage from very high to very low values occurs in a narrow depth range around 4700 m (Bramlette, 1961). Bramlette named this depth the calcite compensation level, which is that depth below which little or no $CaCO_3$ accumulates on the ocean floor. The compensation depth therefore represents the level at which the rate of supply of carbonate organisms (the biological factor) and their rate of dissolution (the physico-chemical factor) are in balance.

Since then, the calcite compensation level has been studied by many investigators. Peterson (1966) suspended calcite spheres at even depth intervals on a taut-wire mooring in the central Pacific. He found a rapid increase in the rate of dissolution at a depth of about 3700 m. Berger (1967) exposed foraminiferal ooze along the same mooring as that of Peterson, and reported pronounced stepwise increases in solution at 3000 m and at 5000 m.

The fact that appreciable solution in calcite occurred above the compensation depth led Berger (1968) to define the lysocline - that depth at which the maximum change in the dissolution of a given foraminiferal assemblage occurs. This level lies at varying heights above the compensation depth. Berger (1968) determined the lysocline of the South Atlantic from the solution of planktonic foraminifera, and mapped it on the basis of the 2° C isotherm. He also identified the lysocline in the southeast Pacific (Berger, 1970). Heath and

Culberson (1970) showed that the calcite compensation level results from a linear increase with depth below the lysocline of the rate of calcite dissolution.

Maxwell et al. (1970) found that in the South Atlantic the $CaCO_3$ content decreases with distance from the crest of the Mid-Atlantic Ridge in each stratigraphic interval of the Cenozoic. This fact suggests progressive subsidence below the compensation level as the crust spread from the ridge crest. In addition, differences in the $CaCO_3$ content of the sediments in different stratigraphic intervals of the Tertiary caused them to suggest that either the absolute depth of the compensation level varied, or the elevation of the ridge crest varied in different epochs, or both. They concluded that major changes in the elevation of the Mid-Atlantic Ridge were responsible for the changes in past carbonate deposition. Therefore, tectonic changes in the depth of the sea-floor constitute a complicating factor in the determination of the calcite compensation level.

This study is concerned with the calcite compensation depth and the concentrations of calcium carbonate, opal and quartz in the surface sediments from the South Atlantic Ocean. By restricting the study to the core-tops, which are assumed to be Holocene, tectonic complications in determining the compensation level can be avoided. In addition, the complicating effects of the glacial periods can be ignored.

This study has been restricted areally (Figure 1) as well as chronologically. Samples well away from the coastline have been used to avoid the high terrigenous input to the continental shelves. Similarly, only samples from the northern and eastern periphery of the Argentine Basin have been included because a non-biologic component derived from the south dominates in most of the basin.

In order to determine the calcite compensation level, cores were used from depths ranging from 733 m to 6020 m, but with a depth bias between 3000 m and 5000 m. A full range of depths is also present for the samples from each of the three major basins. The few Argentine Basin samples are considered as part of the Brazil Basin samples in this study. A "basin" is defined as including not only the deep abyssal area but also the contiguous ridge provinces up to the crest of the ridge.

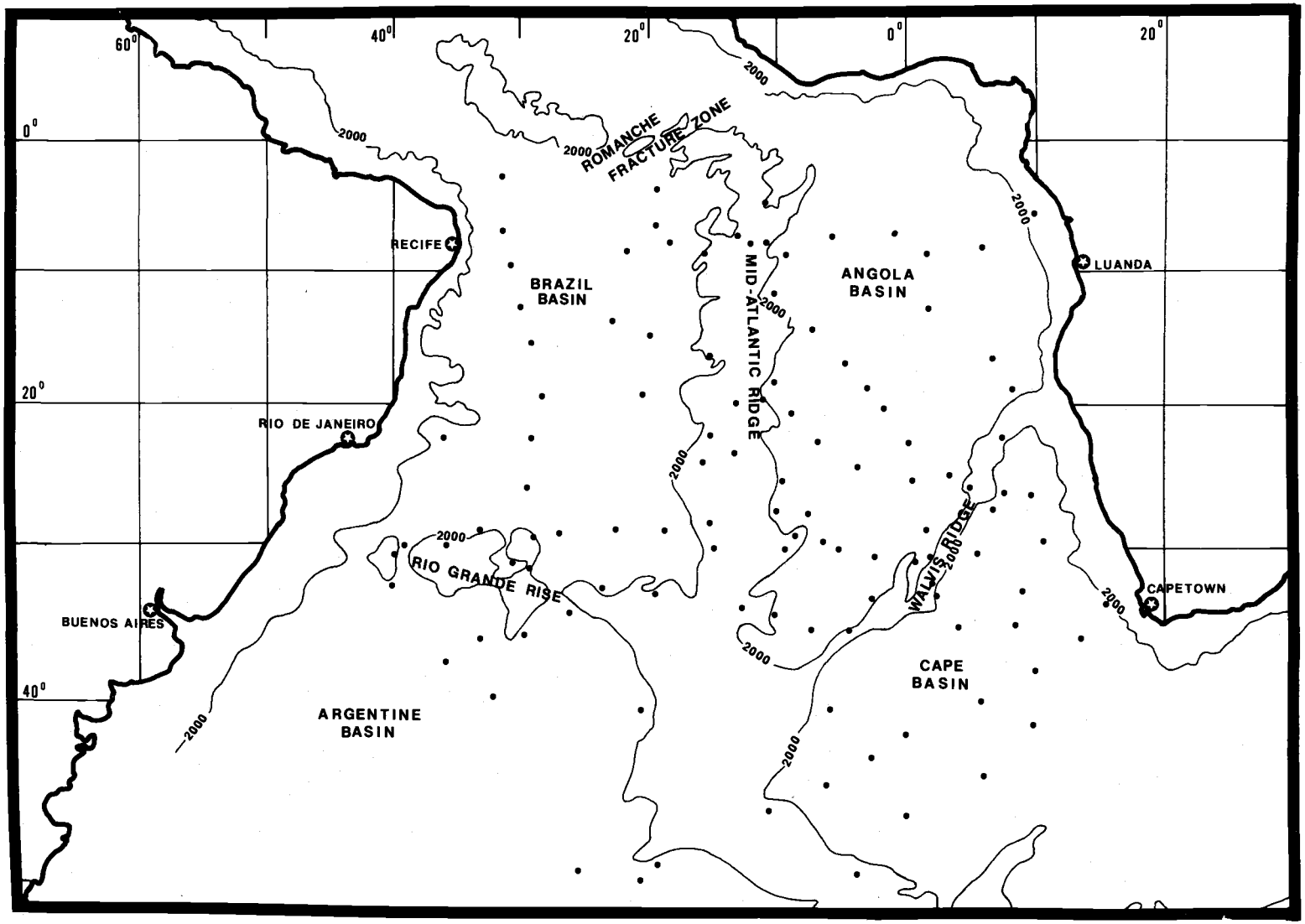

Figure 1. Sample locations (dots). 2000 contour is in fathoms.

CARBONATE METHOD

Calcium carbonate percentages were determined using the WR-12 furnace of the Laboratory Equipment Corporation (LECO). Approximately one gram of the total sample was apportioned for carbonate analysis. This fraction was treated with 10 ml of 10% H_2O_2 for three successive days to destroy the organic material.[1] The sample was then washed into a Teflon evaporating dish and dried overnight at 100° C. The dry sample was ground thoroughly and dried again at 100° C for at least one hour before weighing. After thorough mixing, between 80 and 90 milligrams were weighed onto tared tin foil (which had been washed with reagent grade acetone, rinsed with 95% ethanol, and dried for a minimum of two hours at 100° C). The sample was wrapped in the tin foil which in turn was tamped in a LECO crucible, thereby avoiding any loss of sample upon combustion. Prior to being used, the LECO crucibles were heated at 1150° C for at least eight hours in order to burn off any carbon deposits.

All samples were run in duplicate; if the two readings varied by more than one percent $CaCO_3$, two more determinations were

---

[1] Subsequent tests at Oregon State have shown that this method leaves some organic material. However, for oceanic samples, the differences in $CaCO_3$ content are not significant.

made. Due to insufficient material, four of the 113 samples had a final value based upon readings which differed by more than one percent. The percentage calcium carbonate was calculated by multiplying the LECO digital readout of total carbon by 8.333 (the molecular weight of $CaCO_3$ divided by the molecular weight of carbon).

OPAL METHODS

Methods for determining the percentages of biogenic silica in sediments include infrared spectroscopy, chemical dissolution, and X-ray diffraction.

Chester and Elderfield (1968) determined opal using an infrared technique. However, simple and rapid determination of opal is possible only if the sample contains less than 5% quartz. Moreover, for samples in which the quartz : opal ratio is greater than 1 : 3, "... it is not possible to establish the presence of opal." In order to positively identify opal, a long trial and error modification is necessary. Only 10% of the samples in this study contained less than 5% quartz; furthermore, more than 80% of the samples had a quartz : opal ratio of greater than 1 : 3. Therefore, the infrared technique is unsuitable for large numbers of samples, unless they come from an area of very low quartz concentrations.

Hashimoto and Jackson (1960) contended that amorphous silica could be determined by rapid dissolution in 0.5 N NaOH. After centrifugation of the dissolved sample, they found the amount of silica in the solute spectrophotometrically and repeated the dissolution procedure on the residue. The major question concerning this technique is the number of solutions necessary to completely extract the amorphous silica.

Therefore, the process was tested as follows. Flake form NaOH (10.0020 g) was dissolved in a 500 ml flask with distilled water. Following dissolution, it was rapidly transferred to a plastic bottle. Fifty mg of powder-dry, pure opal were placed in a Teflon beaker, and 50 ml of the NaOH was added. The first extraction required 11 minutes to come to boiling due to an initially cold hot plate and the lack of a cover glass over the beaker. Prior heating of the hot plate and the use of a cover glass reduced the heating time to 5 minutes for all subsequent dissolutions. The beaker was partially immersed in a water bath to cool the sample, which was then centrifuged at 2000 RPM for 5 minutes. The supernatant liquid was stored for analysis, while the solid residue was rinsed into the Teflon beaker with the next 50 ml increment of NaOH. Hashimoto and Jackson (1960) recommend immediate spectrophotometric analysis for silica due to precipitation of aluminosilicates. With a pure opal sample, however, no precipitation occurred.

After four runs, an appreciable quantity of solid opal still remained. Drying and weighing of this residue showed that it was one-third of the weight of the original sample. Therefore, four more dissolutions were made at the end of which a small amount still remained. Spectrophotometer readings showed a total of 83 mg of Si in the eight solutes, whereas the original sample contained only 50 mg. Analysis of the normal distilled water available and used for

NaOH dissolution showed a very significant percentage of dissolved silica: 3.6 mg per 50 ml.

After subtracting this amount, the following results were obtained:

Run	Milligrams of SiO_2	Percentage of Total
1	29.0	54
2	6.1	11
3	6.3	12
4	5.1	9
5	3.1	6
6	1.9	4
7	1.9	4
8	0.7	1

A second opal sample gave the following results:

1	31.7	62
2	11.6	23
3	4.4	9
4	3.4	7

Because of the necessity for so many dissolutions and the requirements for water purity, this technique was found to be inefficient. However, a chemical technique of a double extraction with

five percent sodium carbonate has been used by others (Lisitzin, 1971).

Therefore, the X-ray diffraction technique of Goldberg (1958) and Calvert (1966) was used to ascertain the concentrations of biogenic silica in the samples. However, modifications in the sample treatment were required in order to obtain a reproducible standard curve.

Goldberg (1958) found that upon heating, X-ray amorphous opal converted to cristobalite, which can be measured by X-ray diffraction. He treated sponge spicules (opal source) with a mixture of perchloric and nitric acid and reported the optimum time-temperature combination for conversion to be four hours heating at 900° C.

Calvert (1966) removed carbonate with hot concentrated nitric acid when preparing an opal standard curve (from diatomaceous earth) and with hot 10 percent HCl for the regular samples. He "determined empirically" that optimum conversion occurred at a combination of 1000° C and four hours. In addition, he compared the cristobalite peak heights to those of an internal standard - Al_2O_3. Calvert obtained a peak height ratio of cristobalite to alumina of approximately seven for pure opal.

Attempts to reproduce the foregoing results with opal samples treated with 2N HCl were unsuccessful. Samples were heated to all possible combinations of 960°, 980°, 1000° and 1020° C and 3, 5, 7

and 9 hours. Very little conversion to cristobalite occurred. A new matrix consisting of 1060°, 1080°, 1100° and 1120° C and 6, 8, 10 and 12 hours was tried. Although cristobalite conversion doubled, the peak height ratios were still less than one-tenth of those found by Calvert (1966).

In view of the above discrepancies, tests were made to determine the effects of acid treatment on the conversion of opal to cristobalite. The opal source for these tests as well as for the standard curve was a Scripps South Pacific core, RIS 32P, 0°09' S, 85°59' W (2770 meters). The sample was sieved at 62 μ using only water agitation. The greater than 62 μ fraction contained abundant foraminifera, which were separated from the siliceous organisms by progressive decantations. The presumed opal was treated with acetic acid buffered to pH 5 by a solution of 1 N sodium acetate. After resieving at 62 μ, microscopic examination showed organic matter, many fine (< 62 μ) mineral grains, and dirt trapped in many radiolaria. Therefore, the opal was subjected to two to four minutes of agitation in a Bransonic ultrasonic bath. After resieving, the sample changed color from dark green to light pink and white. A second microscopic examination showed no mineral grains, a much reduced amount of organic matter, and less than one percent radiolaria with entrapped dirt. When the sample was dried at 110° C, the remaining organic matter stuck to the side of the evaporating dish

and was removed. Asymmetric tumbling for 20 hours resulted in a homogeneous sample of 35 grams.

A portion of the opal was treated with boiling 15.7 M nitric acid, another portion with boiling 10 percent hydrogen peroxide, and a third opal portion was not further acidified. After candle-filtering for acid removal and drying, each of the above portions was split to compare the effects of mechanical grinding in water versus n-butanol. The non-acidified, water ground sample was again split to check any differing effects in blending of sample and alumina. They were combined dry, under acetone, and under benzene. Samples were heated at 1000° C for six hours and 1080° C for 12 hours, and then X-rayed. In addition, a portion of the non-acidified, water ground, acetone blended sample was X-rayed without heating as a blank. The opal sample used to test the Hashimoto and Jackson extraction technique (see above) was not acidified and was ground in n-butanol.

The tests resolved the variables as follows:

1. The samples with no acid treatment, other than the buffered acetic acid, converted to cristobalite far more completely at 1000° C than any of the other splits. At 1080° C, the non-acidified and H_2O_2-treated samples showed equal amounts of conversion, with the peak-area ratios very close to the peak-height ratios of Calvert (1966). The peak-area ratios of samples treated with nitric acid

were very close to those from the hydrochloric acid treated samples. Since less conversion resulted from stronger acids, only acetic acid was used on the actual samples.

2. The samples ground in water always converted more completely than those ground in n-butanol, regardless of the acid treatment.

3. The samples blended under acetone and benzene produced appreciably more conversion than the dry blended sample; the benzene inhibited conversion slightly compared to acetone.

4. The samples heated at 1080° C always converted more completely than those heated at 1000° C.

5. The unheated opal blank showed no conversion.

After taking these results into account, the following procedure was adopted:

1. Carbonate was removed by addition of acetic acid (buffered as above) until effervescence ceased or until all foraminifera were dissolved.. Samples were heated at 80° C and agitated to increase the rate of dissolution.

2. The presence of acetic acid enhanced flocculation; therefore, the samples were allowed to settle and the excess liquid siphoned off and replaced with distilled water until flocculation ended.

3. The samples were candle-filtered three times with distilled water, the second time with boiling water.

4. The samples were ground for two hours in a mechanical grinder (Fisher no. 8-323) under the minimum quantity of distilled water necessary to maintain wetness. Excess water caused a reduction in peak intensity; insufficient water resulted in dryness followed by very high temperatures and too great a peak intensity.

5. Samples were transferred to evaporating dishes and dried at 100°-110° C.

6. The dry samples were homogenized by grinding by hand with a Diamonite mortar and pestle. This was necessary to avoid variations in peak intensity due to size separation while settling and drying.

7. A portion of the sample sufficient to fill an X-ray planchet (0.4 g) was blended under acetone with one-half of its weight (within 0.1 mg) of internal standard (0.2 g). The internal standard was WCA α-Al_2O_3 microgrit (size three) which had been previously heated to 1000° C for 12 hours.

8. When dry, the blended sample was transferred to an Alundum crucible and placed in a preheated oven at 1000° C for 24 hours. The combination of 1000° C and 24 hours produced peak-area ratios slightly less than those of 1080° C and 12 hours, but lower temperature reduced the possible conversion of clay minerals to cristobalite, a danger which is present around 1100° C.

9. The heated sample was reground three times under acetone,

powdered with a stiff brush, and pressed on a torque wrench equivalent to 25 psi in an aluminum X-ray planchet. When the total sample was much less than 0.6 g, instant coffee backing was used in the planchet.

10. The sample was X-rayed using a Norelco X-ray diffraction unit with automatic sample changer and monochromator, and under the following specifications:

Radiation - Cu K monochromatized by means of a curved graphite crystal diffracted-beam monochromater

Tube Voltage - 35 kv

Tube Current - 25 ma

Divergence Slit - 1°

Receiving Slit - 0.1 mm

Scale Factor - 2000

Time Constant - 4

Goniometer Speed - 1/16°/min

Chart Speed - 1/4 inch/min

The area under the cristobalite (101) peak (4.09 Å), was computed automatically by a Canberra digital control and data processing system. After subtraction of background area, this figure was divided by the computed area under the Al_2O_3 (012) peak (3.48 Å) minus its background. By referring to the opal standard curve (Figure 2), the percentage opal in the sample was determined.

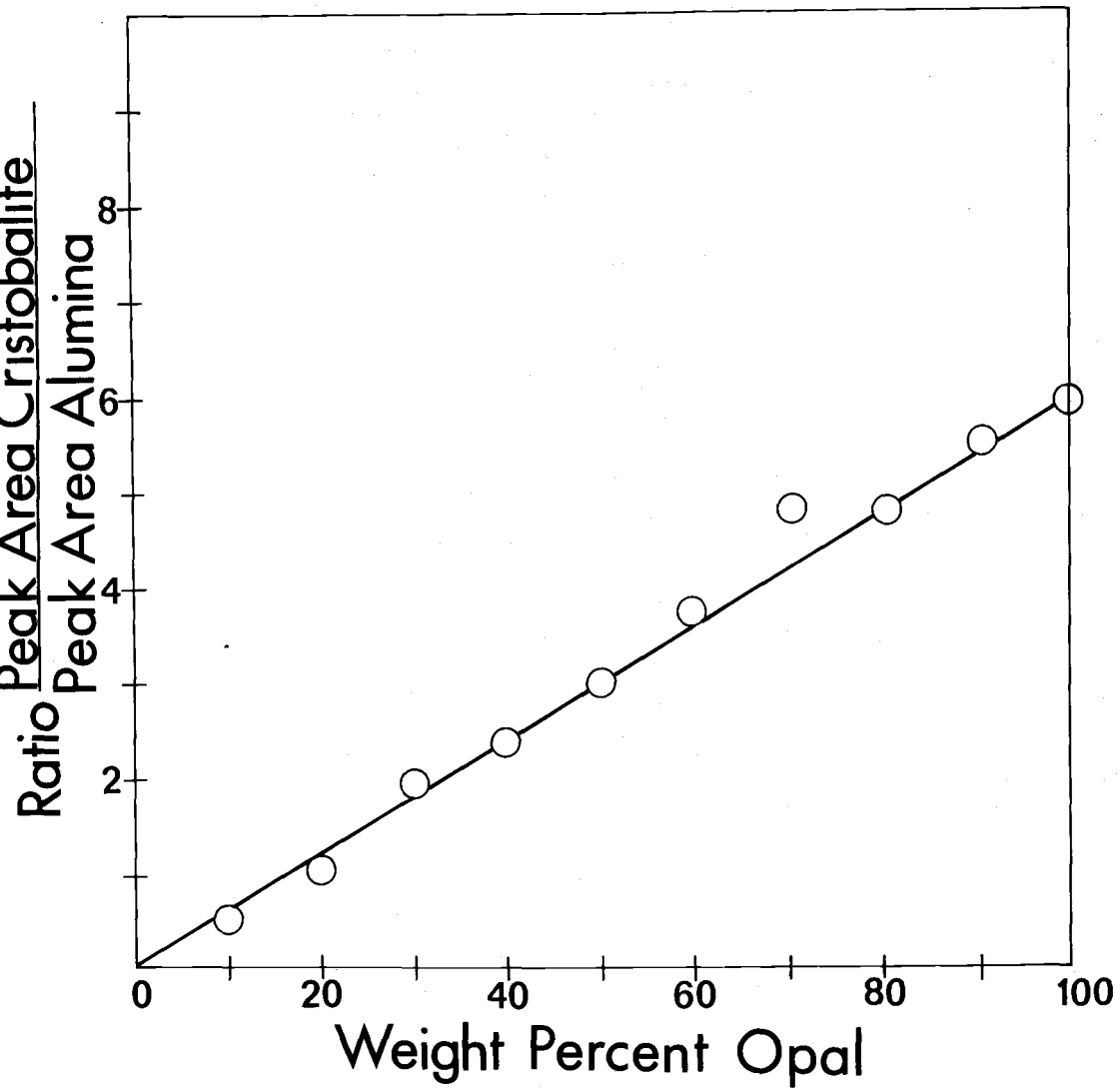

Figure 2. Opal standard curve.

The standard curve was prepared by mixing the pure opal described above with an opal-free matrix in known amounts. The matrix was montmorillonite 23 (bentonite) from Chambers, Arizona (Ward's Scientific Establishment no. 48 W 1230 clay mineral standard). The montmorillonite was mechanically ground in water for two hours, then dried and homogenized. A montmorillonite blank heated for 25 hours at 1000° C showed no cristobalite conversion.

The standard curve has a slope of 0.6 and is reliable to ±5 percent. The deviation of the point at 70 percent opal caused no difficulty because only one sample contained more than 57 percent opal, and it fell above 80 percent.

QUARTZ METHOD

The opal samples were simultaneously X-rayed for quartz. Calvert (1966) X-rayed the samples prior to heating for cristobalite. However, Till and Spears (1969) showed that heating at 950° C removed the interference from clay peaks, as well as increased the relative intensity of the quartz peaks. Therefore, only one X-ray run is necessary. The area under the 3.34 Å quartz peak (101) was computed by the Norelco unit and compared with the 3.48 Å α-Al_2O_3 (012) peak, exactly as in the opal method.

Standard quartz was prepared by grinding optical quality "Brazil" quartz in a mechanical grinder. No size separation was made since none was made on the samples. Mixtures of standard quartz and montmorillonite (bentonite 23) at 10 percent intervals from 10 to 100 percent were X-rayed with Al_2O_3 as an internal standard.

A plot of peak area ratios versus percentage quartz (Figure 3) shows a straight line from 0 through 50 percent. The points between 60 and 100 percent quartz form a line of much steeper slope which intersects the low percentage line at 55 percent. Since only one sample contained more than 55 percent quartz, the straight line through the origin was used.

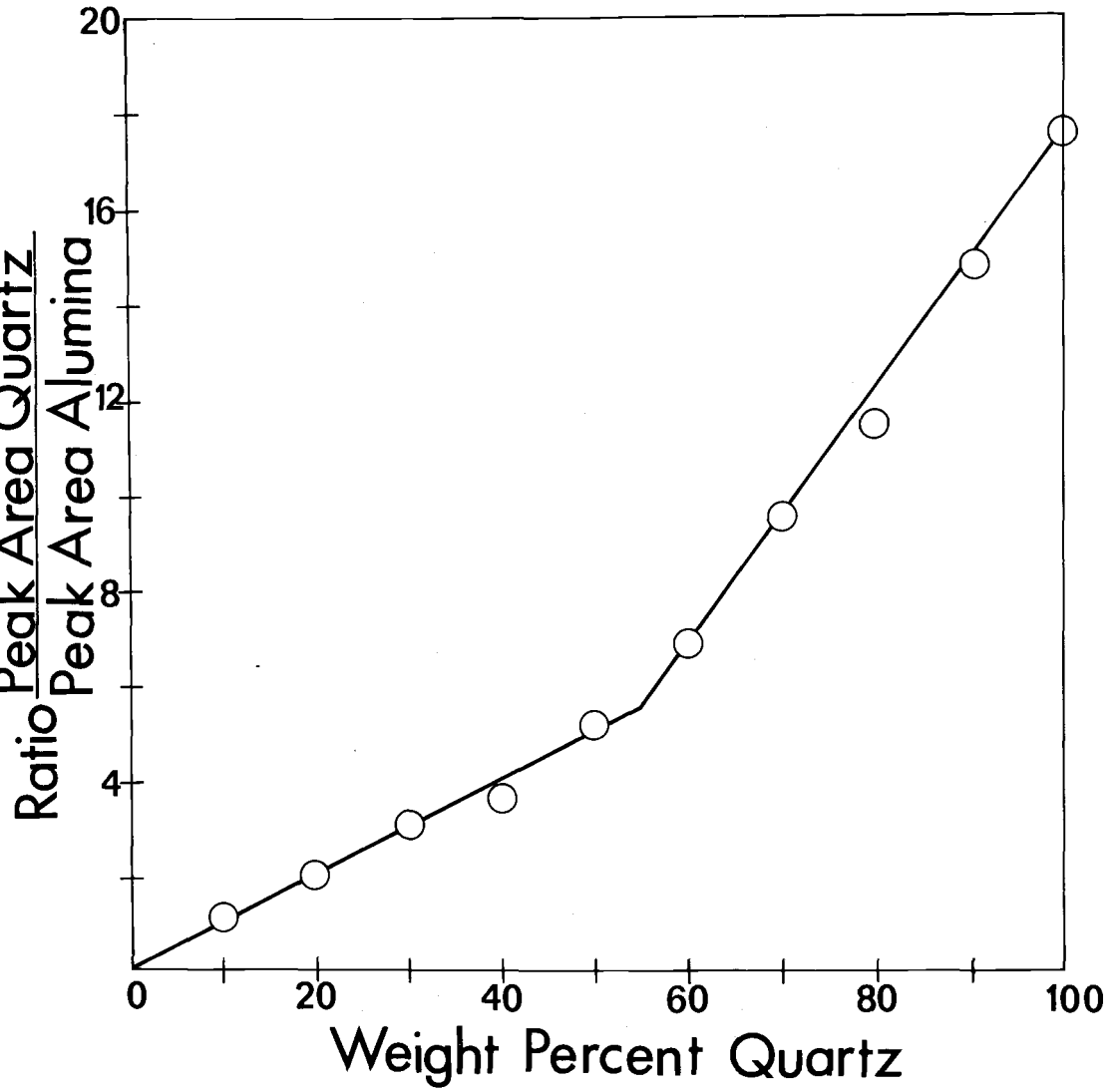

Figure 3. Quartz standard curve.

CARBONATE DISTRIBUTION

The concentrations of calcium carbonate are mapped in Figure 4. The stars indicate locations of additional data points supplied by K. K. Turekian. Three locations are surrounded by diamonds; these are local topographic highs for which contouring is unjustified.

Figure 4 illustrates the influence of bottom water circulation in greater detail than previous maps, without change in the main features. The ridge areas are very high in $CaCO_3$, while the deep basins are low. The southernmost Mid-Atlantic Ridge sites, however, are quite low compared to those farther north. The $CaCO_3$ pattern in this region is produced by an inclined northward dipping compensation level intersecting the ridge. This is in agreement with Berger (1968), who found that the lysoclinal depth increased from south to north, and with Kennett's (1966) observation of a very shallow (500 m) compensation depth in the Ross Sea. Another possibility, a paucity of planktonic foraminifera living in the area, is disproved by a map of their absolute abundance in surface waters of the Atlantic (Be and Tolderlund, 1971). The number of specimens increases to the south of 40° S.

To the west of the Mid-Atlantic Ridge, the Antarctic Bottom Water (AABW) flows through breaches in the Rio Grande Rise into the Brazil Basin. Burckle and Biscaye (1971) found two passageways

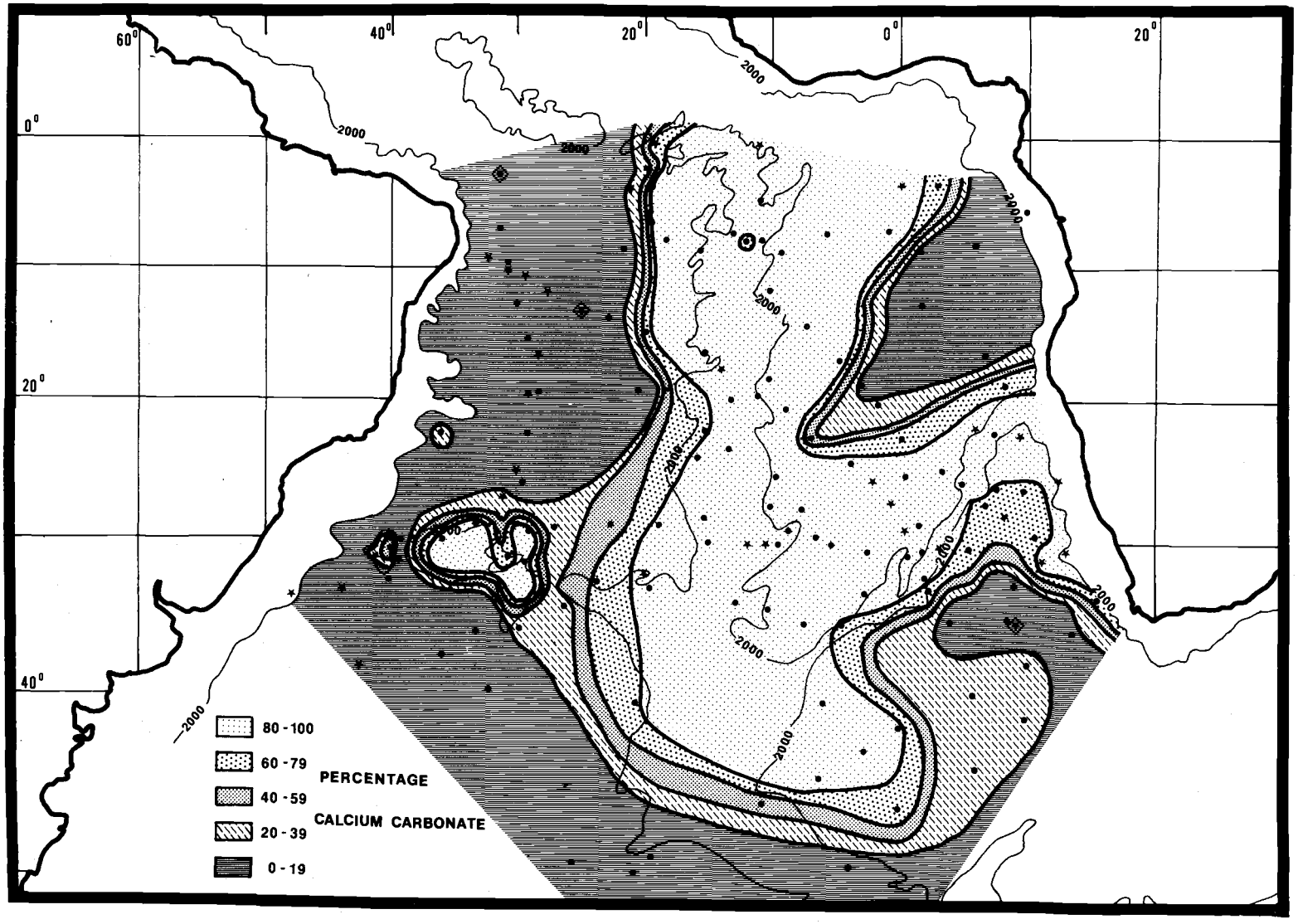

Figure 4. Calcite concentration map (as a percentage of the total sample). Stars indicate additional data from K. K. Turekian.

for AABW through the Rise. The map illustrates these two channels perfectly. The Vema Channel at 39° W is the primary breach, and very low $CaCO_3$ values are found there. The Hunter Channel at 26° W is a secondary gap, and the $CaCO_3$ values are correspondingly somewhat higher due to lower volume influx of AABW.

The AABW flows along the western side of the Brazil Basin, while warmer North Atlantic Deep Water is deflected to the east (Olsen, 1968). This disparity, allied with an east-west depth gradient, produces an east-west $CaCO_3$ content gradient. The AABW flows eastward through the Mid-Atlantic Ridge at the Romanche Fracture Zone; the $CaCO_3$ contours are also deflected to the east. However, the coldest Brazil Basin water is excluded from the Fracture Zone by its 4300 m sill. The deepest Romanche Gap water is 0.5° C (potential temperature) warmer than the deepest Brazil Basin water (Olsen, 1968).

In the Angola Basin, the lowest $CaCO_3$ values occur in the northeastern part of the basin, which is also the deepest and coldest area. This might be due to influx of AABW, but this is also the region which receives terrigenous output from the Congo River. In the absence of a low carbonate zone connecting the deep basin with the Romanche Fracture Zone, it seems more probable to attribute the low $CaCO_3$ content to dilution than to solution. However, microscopic examination of CIRCE 216 revealed extensive smoothing

and holing of foraminiferal tests, as well as many fragments. Moreover, Edmond (1970) found significant lateral mixing of AABW from the north at the same station and reported, from a salinity balance calculation, that Angola Basin waters below 3000 m have an AABW component of 15-20 percent. Some dissolution is taking place, therefore, but dilution is probably the dominant factor.

Cold water is prohibited entry to the southern Angola Basin by the Walvis Ridge; on the other hand, warm (2.4° C) Angola Basin water overflows a 3000 m sill into the Cape Basin (Olsen, 1968). It mixes there with water which has come from the Atlantic-Indian Basin by way of the Agulhas Basin (southeast of the Cape Basin). The Angola Basin water probably transports carbonate-rich sediments south from the Walvis Ridge and deposits them in the contiguous area. The deeper portion of the Cape Basin farther to the south presents a situation similar to that of the northeast Angola Basin. As it is deep, it is close to the compensation level, but it is also the area most likely to receive turbidites from southwest Africa. However, no estimate can be made as to which is the controlling factor.

OPAL DISTRIBUTION

The map of concentrations of carbonate-free opal (Figure 5) bears a large-scale resemblance to the Meteor map of standing crop of planktonic organisms (Hentschel, 1933). Hentschel also prepared maps of the components of the total standing crop; the opal map correlates most closely with that for diatoms.

Figure 5 does not correspond well to productivity maps between 20° and 30° S and from the African coast to the Mid-Atlantic Ridge. However, the pattern here is determined by rather small differences between samples, differences that are often less than the analytical error. However, opal concentrations are higher to the east than to the west of the Mid-Atlantic Ridge, which is a reflection of the productivity pattern. Other than this difference, the high opal bands at the northern and southern portions of the map are the only uniquely defined patterns on the map.

The absence of very high opal values off the African coast is at first striking, since coastal upwelling might be expected to create high plankton productivity and therefore large opal concentrations. However, Smith (1968) has shown that upwelling takes place within 60 kilometers (35 miles) of the coastline. The cores used in this study are located at least 360 km (200 miles) from shore (except V12-73), and outside the upwelling zone. Lisitzin (1971) illustrates

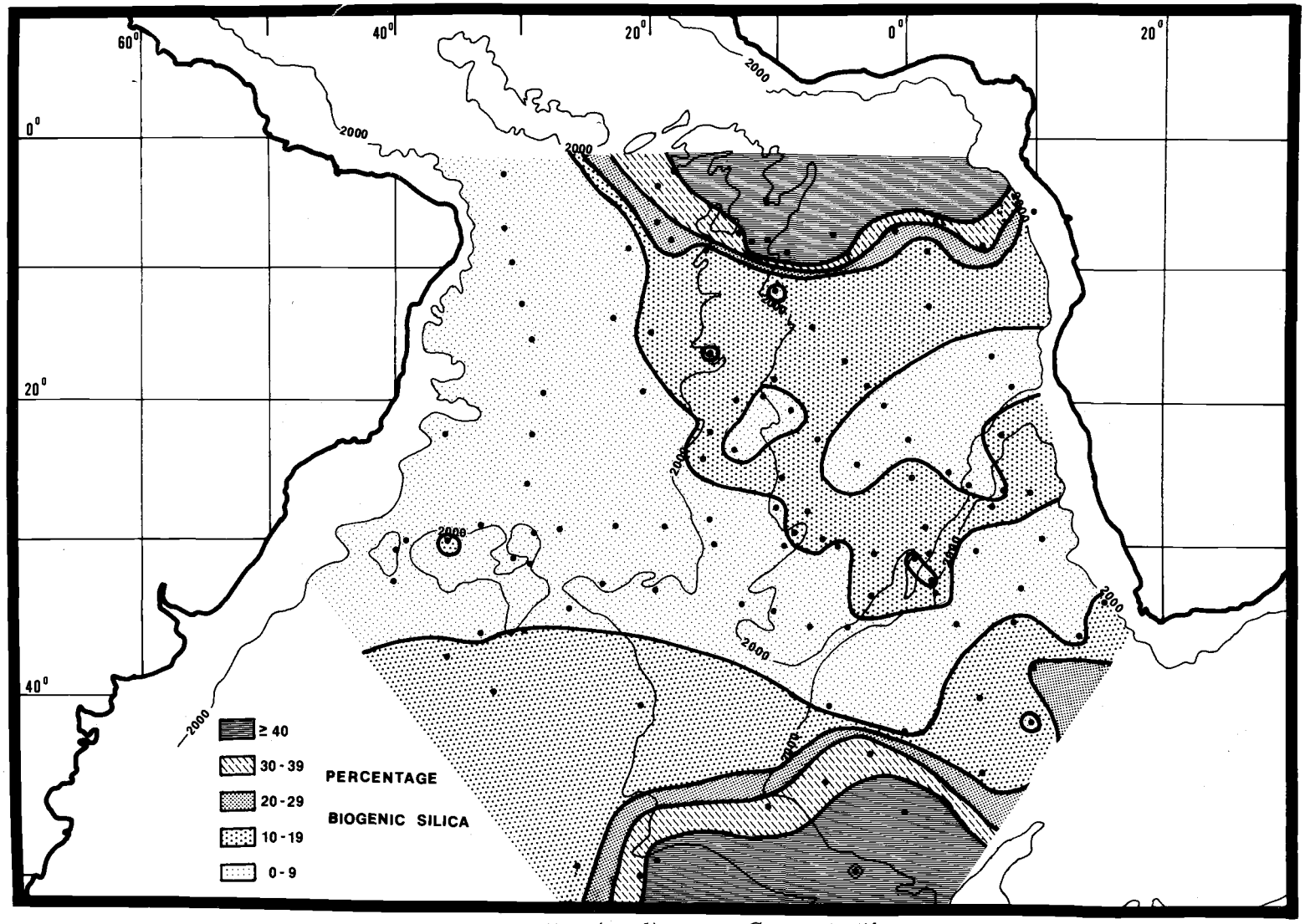

Figure 5. Biogenic silica (opal) map. Concentrations are on a carbonate-free basis.

that high opal values are found off southwest Africa, but only very close to shore.

Comparison of Figure 5 with Figure 6 (opal - percent of total sample) indicates the relative significance of opaline and carbonate sedimentation. The northern band of high opal vanishes, while the southern band is reduced in area. The scale is also reduced by a factor of two. The appearance of a new relative opal high in the Angola Basin is a further effect of low carbonate concentrations.

The maps may be contrasted further by averaging values over intervals of 10 degrees of latitude:

Latitude (°S)	Opal	Opal (% of total)	$CaCO_3$
0-10°	29	6	63
10-20°	8	3	52
20-30°	9	2	73*
30-40°	9	4	57
40-50°	26	13	49

The northern band is reduced by a factor of five, while that in the south only decreases by a factor of two. This disagreement is due to higher opaline productivity in the south, combined with the diminished carbonate dilutions as shown by the 14 percent difference in the $CaCO_3$ concentrations.

---

* Unusually high due to Walvis Ridge and Rio Grande Rise stations.

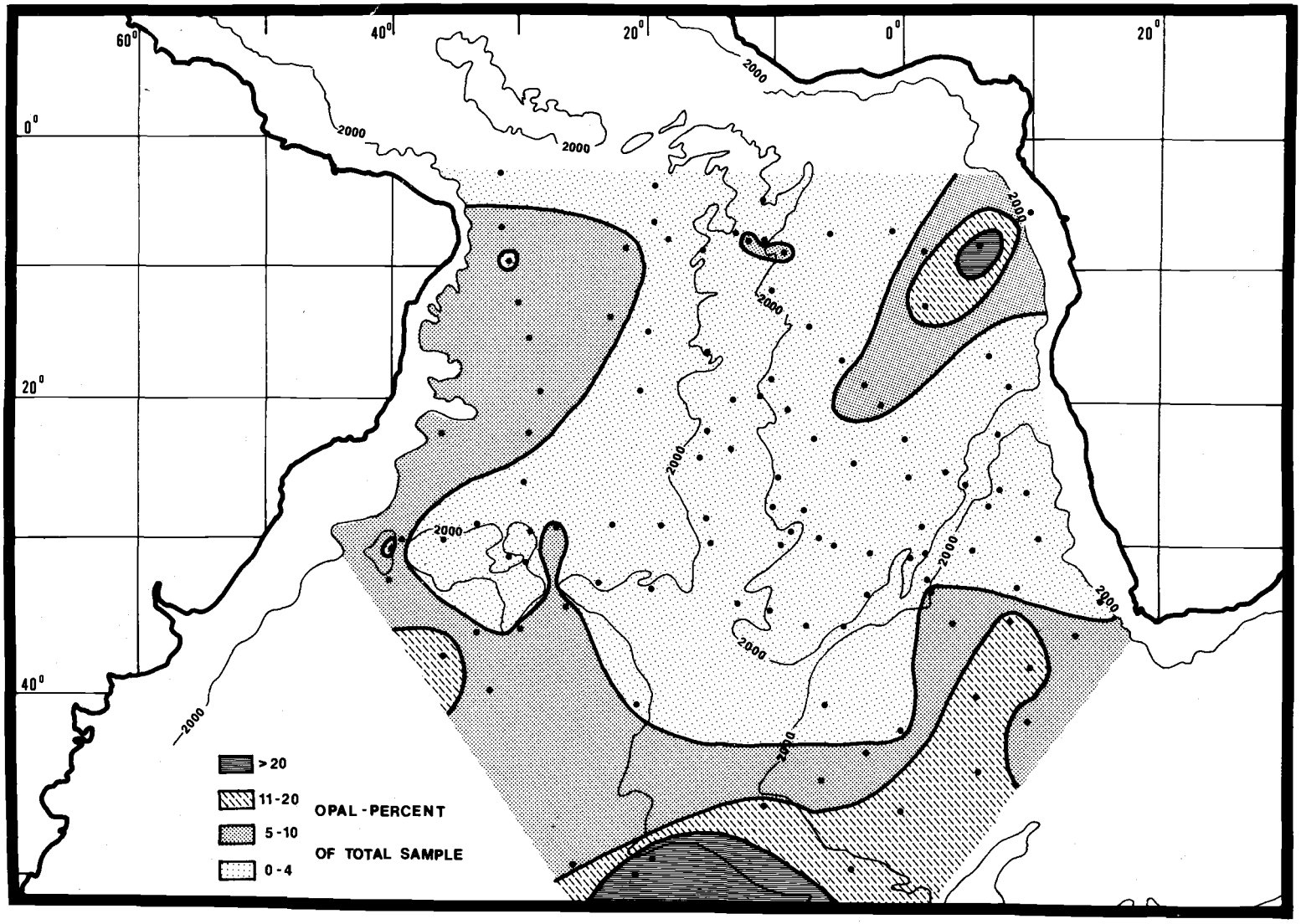

Figure 6. Opal (% of total sample) concentration map.

QUARTZ DISTRIBUTION

Quartz concentrations are generally thought of as indicators of terrigenous supply to deep-sea sediments. Figure 7 (quartz on a carbonate-free basis) shows that this is true to a certain extent in the South Atlantic. Low quartz concentrations are found on and near ridges, while higher values occur closer to shore. Figure 8 illustrates that quartz is not a very significant component of the total sediment, since only four samples contain greater than 20 percent. Figure 8 also reiterates the influence of carbonate sedimentation, as it is essentially a "negative" of Figure 4.

The two major quartz areas to be explained in Figure 7 lie off the southwest coast of Africa and just south of the Rio Grande Rise. The high quartz region off Africa is most easily explained as a combination of terrigenous input and ice-rafted detritus. A map of the U. S. Navy Hydrographic Office (No. 15254, 1961) draws the line for the northern limits of sea ice at about 35° S off the tip of Africa. Ewing et al. (1966) indicate that the area is one in which turbidites are found. A turbidite whose volume decreases with distance from shore coupled with ice-rafted quartz which increases to the south could create a large area of high quartz values like that off the

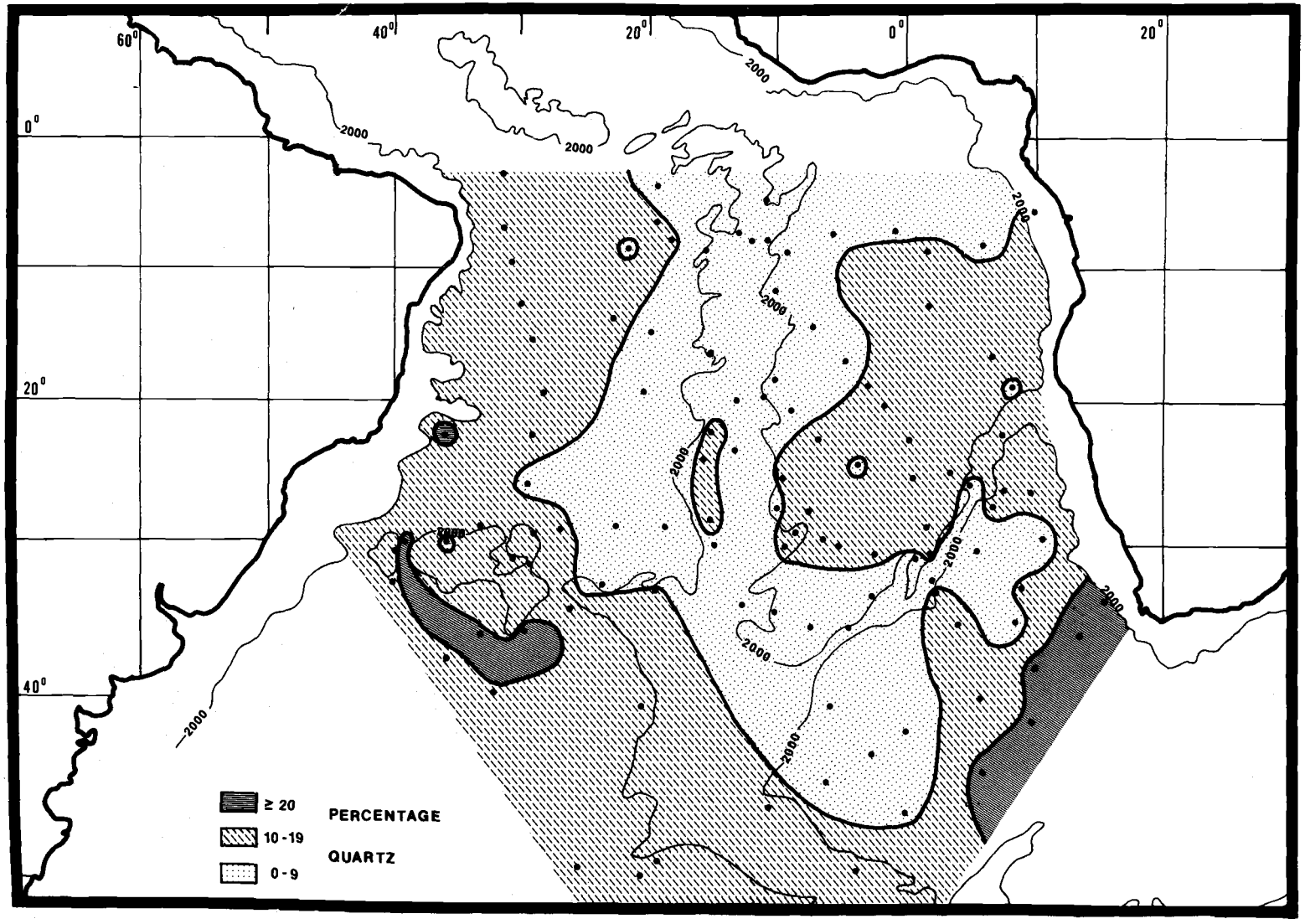

Figure 7. Quartz concentration map on a carbonate-free basis.

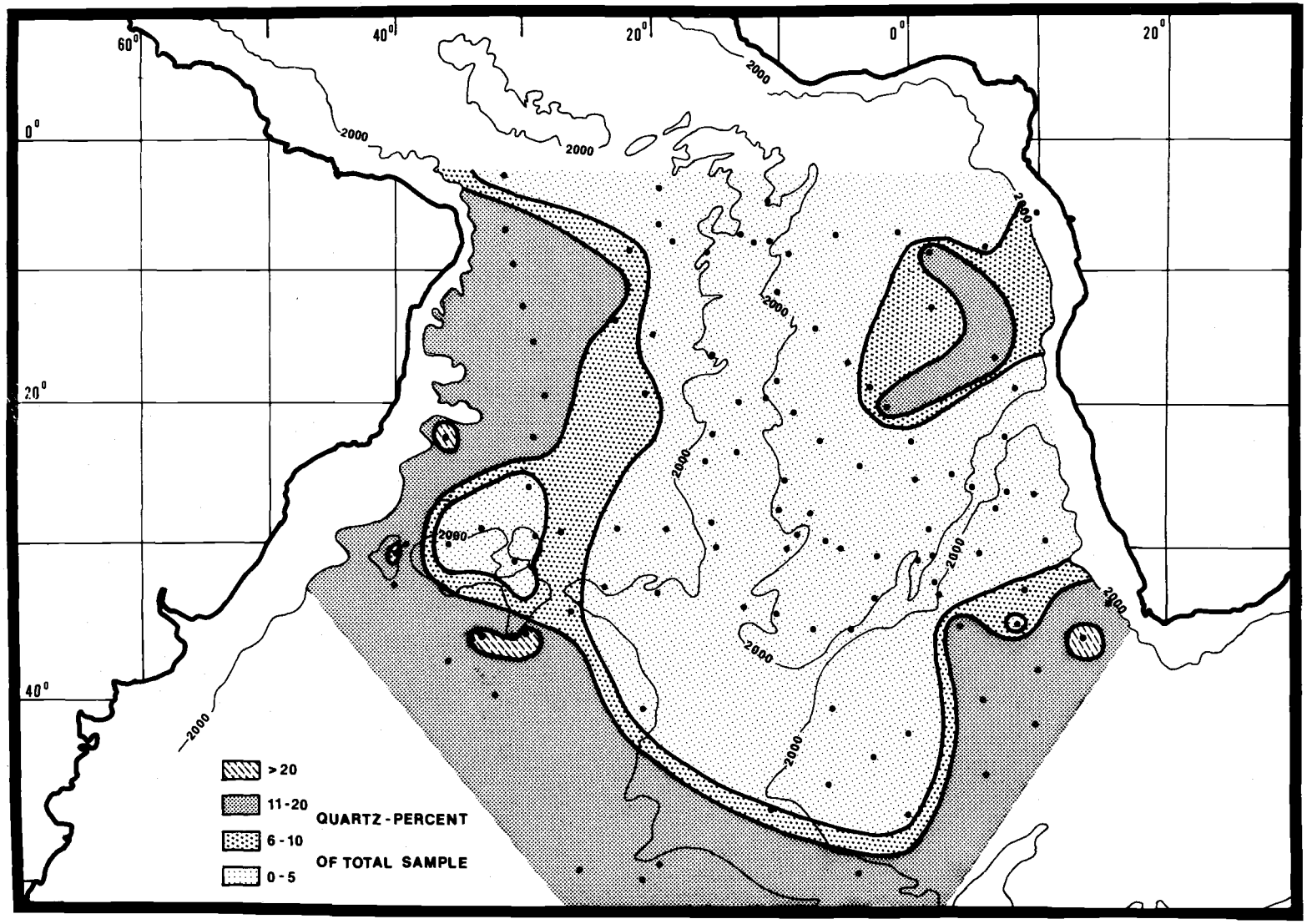

Figure 8. Quartz (% of total sample) concentration map.

African coast. A relatively minor eolian component is also present off the African coast (Arrhenius, 1963), but its magnitude is low compared to the Saharan values at 10° N.

The northern limit of ice-rafting crosses the Mid-Atlantic Ridge at about 40° S and then extends northward to the southern edge of the Rio Grande Rise. The two high quartz points (on Figure 8) south of the Rio Grande Rise are included within the sea-ice area. The main quantity of continental detritus in the Argentine Basin is not derived from South American rivers such as the Rio de la Plata (Biscaye, 1965; Biscaye and Dasch, 1968), but rather from the south of the Basin due to transport by the Antarctic Bottom Water (Jones et al., 1970). In addition, Hollister and Elder (1969) report evidence for a tongue of quartz-rich mud extending from the Weddell Sea into the Argentine Basin, which is caused by transport in the AABW. The high quartz point in the breach of the Rio Grande Rise could easily represent the distal end of this tongue. The other high values could be caused by the addition of ice-rafted quartz to that quartz transported by contour currents. Insufficient sample coverage precludes attempting to map this feature within the Argentine Basin.

CLAY DISTRIBUTION

Clay concentrations were not measured directly, but the residue obtained by subtracting the carbonate, opal, and quartz percentages of the total sample from 100 percent is defined as "clay" (Figure 9).

Biscaye (1964) shows that both kaolinite and illite in the South Atlantic originate as continental detritus. The "clay" map is in accordance with this interpretation, as both high "clay" areas are near land. The Angola Basin "tongue" is probably a result of southward transport from the Congo River, since it has a large outflow, no delta, and topographic contours in the Congo Canyon indicate channelization to the south. Heezen et al. (1964) report that the Congo feeds directly into the Angola Basin. A core from the Congo River mouth (V12-73) contains equal amounts of kaolinite and illite (Dasch et al., 1966), while the clay component off Brazil is predominantly kaolinite (Biscaye, 1965).

The identification of the "clay" residue with clay can be, in part, numerically confirmed. Based upon independently measured clay concentrations, Turekian and Stuiver (1964) published the following clay accumulation rates:

V12-66 - 0.13 g/cm^2/1000 yr

V16-36 - >0.05 g/cm^2/1000 yr (0.07 average)

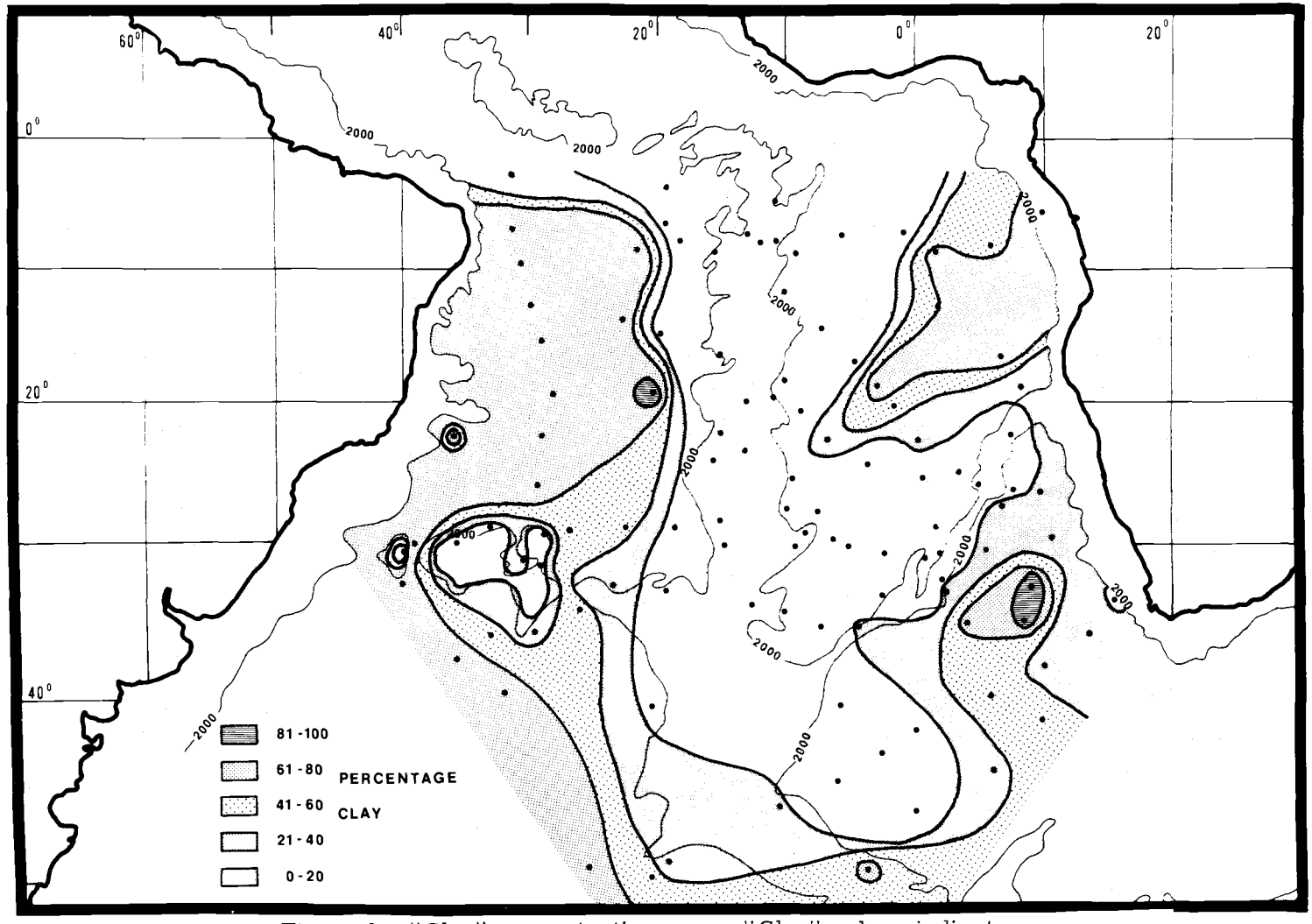

Figure 9. "Clay" concentration map. "Clay" values indicate the difference between the sum of calcite, opal, and quartz and 100%.

The "clay" values for these cores, when multiplied by the accumulation rates and the bulk densities of Turekian and Stuiver (1964), produced these rates:

V12-66 - 0.12 g/cm^2/1000 yr

V16-36 - 0.06 g/cm^2/1000 yr

If the "clay" values illustrate terrigenous input to the sediment, these values would supersede quartz for this purpose due to the significant ice-rafted component in the quartz percentages.

ACCUMULATION RATES

Accumulation rates have been determined by various investigators for 11 South Atlantic cores, which are all included in this paper. Table 1 gives the data in terms of accumulation rates for each of the four components: carbonate, opal, quartz and "clay."

Ku et al. (1968) and Goldberg (1968) use different ways of fitting a rate line to the points in a plot of Th^{230}/Th^{232} versus the depth in core. Here, Goldberg's interpretation has been used because his values are indications of rates in the tops of the cores, whereas the higher rates of Ku et al. are averages for the entire lengths of the cores. The lower rates of Goldberg are in accordance with the sharp decrease in accumulation rates over the last 11,000 years found by Broecker et al. (1958).

The small number of measurements permits only a few conclusions. However, the following generalizations can be made:

1. Carbonate and clay are the only significant components of the total rate.

2. Carbonate rates are low only in the Brazil and Argentine Basins.

3. Opal and quartz rates do not differ significantly.

4. Clay rates are usually 5-10 times those of opal.

5. Carbonate rates, except in the above basins, are usually 5-10 times those of clay.

Table 1. Accumulation rates.

Sample	Total Rate	$CaCO_3$ Rate	$CaCO_3$ free Rate	Opal Rate	Qtz. Rate	"Clay" Rate	Source and Method
LSDA 159	13	8.97	4.0	.44	1.36	2.21	1
LSDA 163	2.2	2.11	.09	.02	.01	.07	1
LSDA 168	1.6	1.47	.13	.02	.02	.10	1
LSDA 178	1.9	1.75	.15	.02	.02	.11	1
LSDA 183	2.0	1.98	.02	.00	.00	.02	1
V 9-11 *	15	10.5	4.5	.23	.45	3.75	2
V 9-16 *	0.8	.05	.75	.06	.06	.62	2
V12-16 *	4.0	.20	3.8	.30	.27	3.20	2
V12-52 *	1.8	.07	1.7	.17	.32	1.22	2
V12-66	23	20.7	2.3	.37	.28	1.61	3
V16-36	13	11.96	1.0	.05	.08	.91	3

All rates are in mm/1000 yr.

Table 1 (Continued)

* Brazil and Argentine Basin samples.

Sources:

1. Goldberg and Griffin (1964): Io-Th
2. Goldberg and Koide (1962): Io-Th
3. Ku et al. (1968): C-14 (from Turekian and Stuiver, 1964)

Sample	Acc. Rate $\frac{cm}{1000\ yr}$	Bulk Density[1]	Acc. Rate $\frac{g/cm^2}{1000\ yr}$
LSDA 159	1.30	.925	1.20
LSDA 163	.22	.967	.21
LSDA 168	.16	1.004	.16
LSDA 178	.19	.893	.17
LSDA 183	.20	.852	.17

[1] A known volume of wet sediment from the upper 10 cm was dried at 100° C and weighed. Shrinkage of the cores, which are kept cold and wet in plastic liners, was measured and found to be negligible.

CALCITE COMPENSATION LEVEL

Brazil and Northern Argentine Basins

Figure 10 shows the calcite compensation level for all points west of the Mid-Atlantic Ridge crest. After drawing a line below which little, if any, calcite content exists, a compensation depth of 4800 meters is indicated. Berger (1968) estimated a lysocline of 4400 meters based upon the almost complete dissolution of foraminifera at 4900 m (which usually occurs at least 500 m below the lysocline). As complete dissolution of foraminifera occurs close to the compensation depth, the 4800 m compensation level found is compatible with Berger's figure of 4900 m.

The scatter in Figure 10 illustrates the diversity of dilutants and of bottom water conditions in the western South Atlantic. The influx of Antarctic Bottom Water coincides with the low $CaCO_3$ values at relatively shallow depths of the southern Mid-Atlantic Ridge and the area contiguous to South America, while the points from the Mid-Atlantic Ridge flank north of the Rio Grande Rise and the Rio Grande Rise itself are high in $CaCO_3$. This contrast is depicted the most vividly by the fact that station V24-248 on the west end of the Rio Grande Rise contains pteropod tests (composed of relatively soluble aragonite), while the three points in the 39° W breach in the Rise contain 1, 5 and 7 percent carbonate.

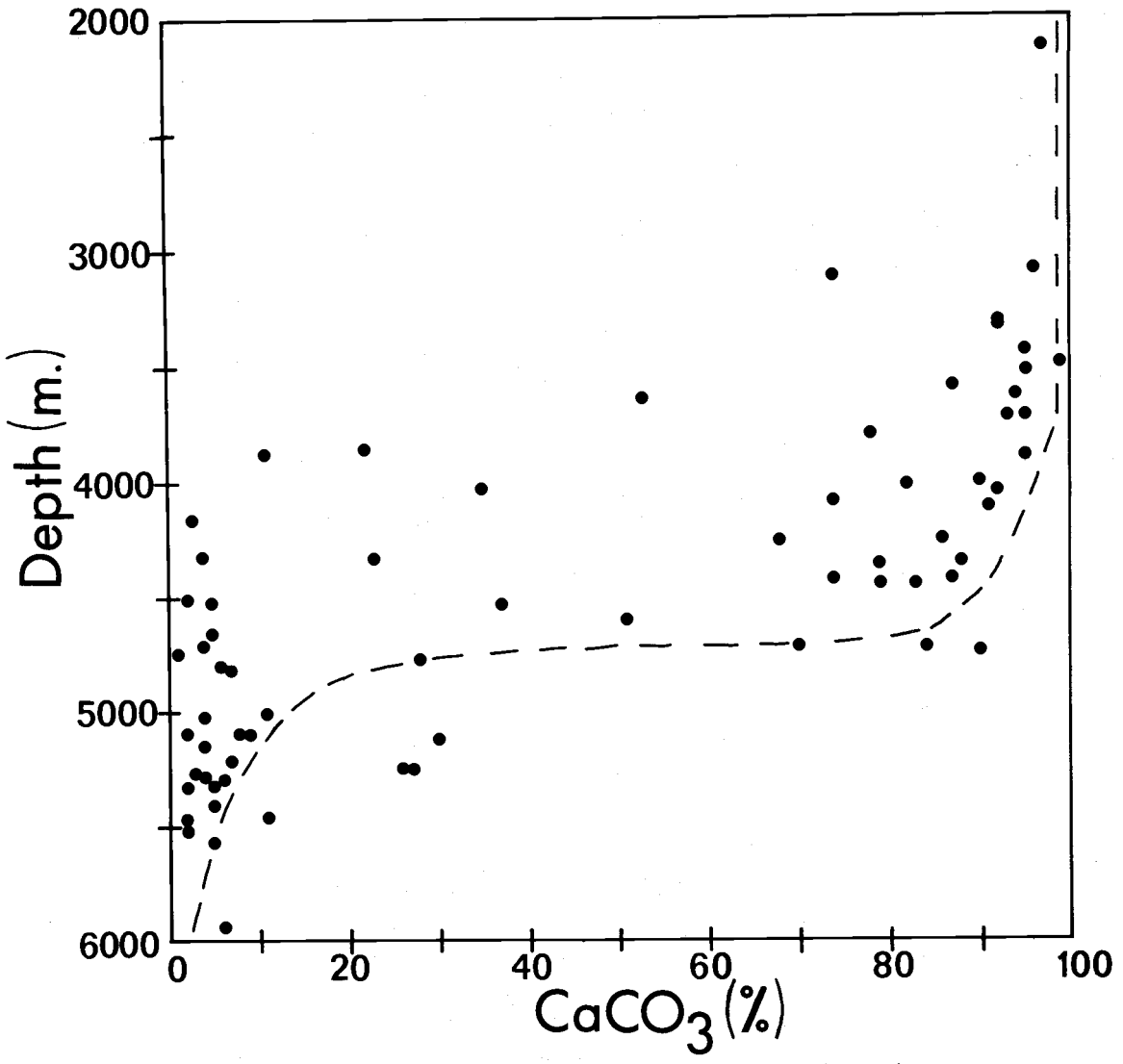

Figure 10. $CaCO_3$ vs. depth - Brazil and northern Argentine Basins. The dashed line indicates the calcite compensation level.

Cape Basin

The Cape Basin samples, as shown in Figure 11, permit a more exact determination of the compensation level than those found in the Brazil and northern Argentine Basins. Only one point contains more than 90 percent $CaCO_3$. This lack of high values is due to the paucity of shallow depth stations from the Walvis Ridge and the Mid-Atlantic Ridge (north of 45° S) allied with the influx of AABW and possibly turbidites.

The calcit compensation level is 5100 meters. Turekian (1964) plots $CaCO_3$ against depth for Cape and Argentine Basin cores. Extraction of the Cape Basin points from the total plot yields an identical compensation depth: 5100 meters.

Angola Basin

As can be seen in Figure 12, a case could be made for the absence of a true compensation level in the Angola Basin. Only one sample contains less than 18 percent $CaCO_3$. The average depth of the line drawn in the figure is 5400 meters. Berger (1968) found the lysocline to lie at or possibly below 5200 meters. The difference between the two depths is at best 200 meters which is far less than the minimum of 500 m assumed by Berger (1968) for the Brazil Basin. Therefore, the 5400 m depth represents a minimum value

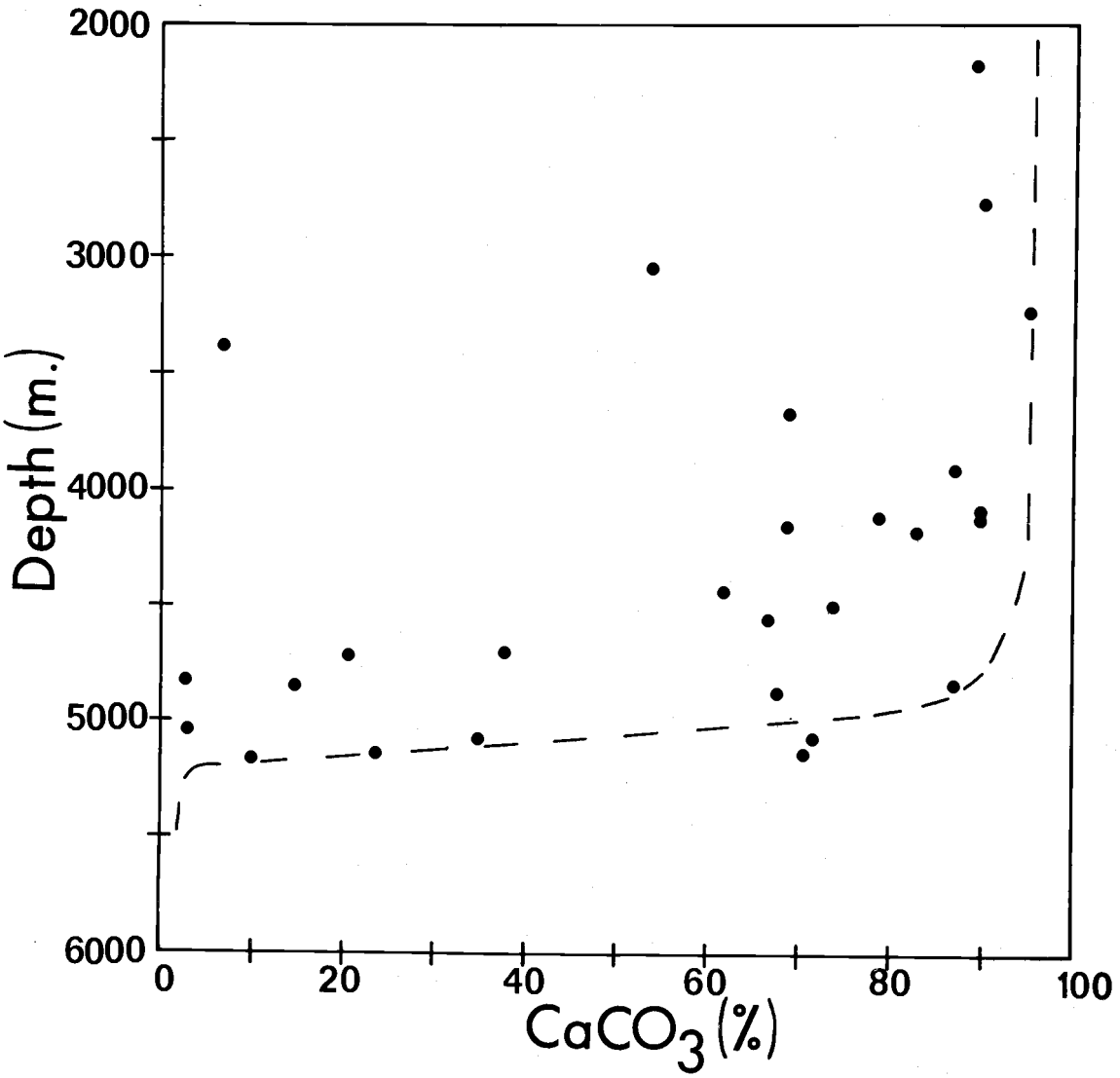

Figure 11. $CaCO_3$ vs. depth - Cape Basin.
The dashed line indicates the calcite compensation level.

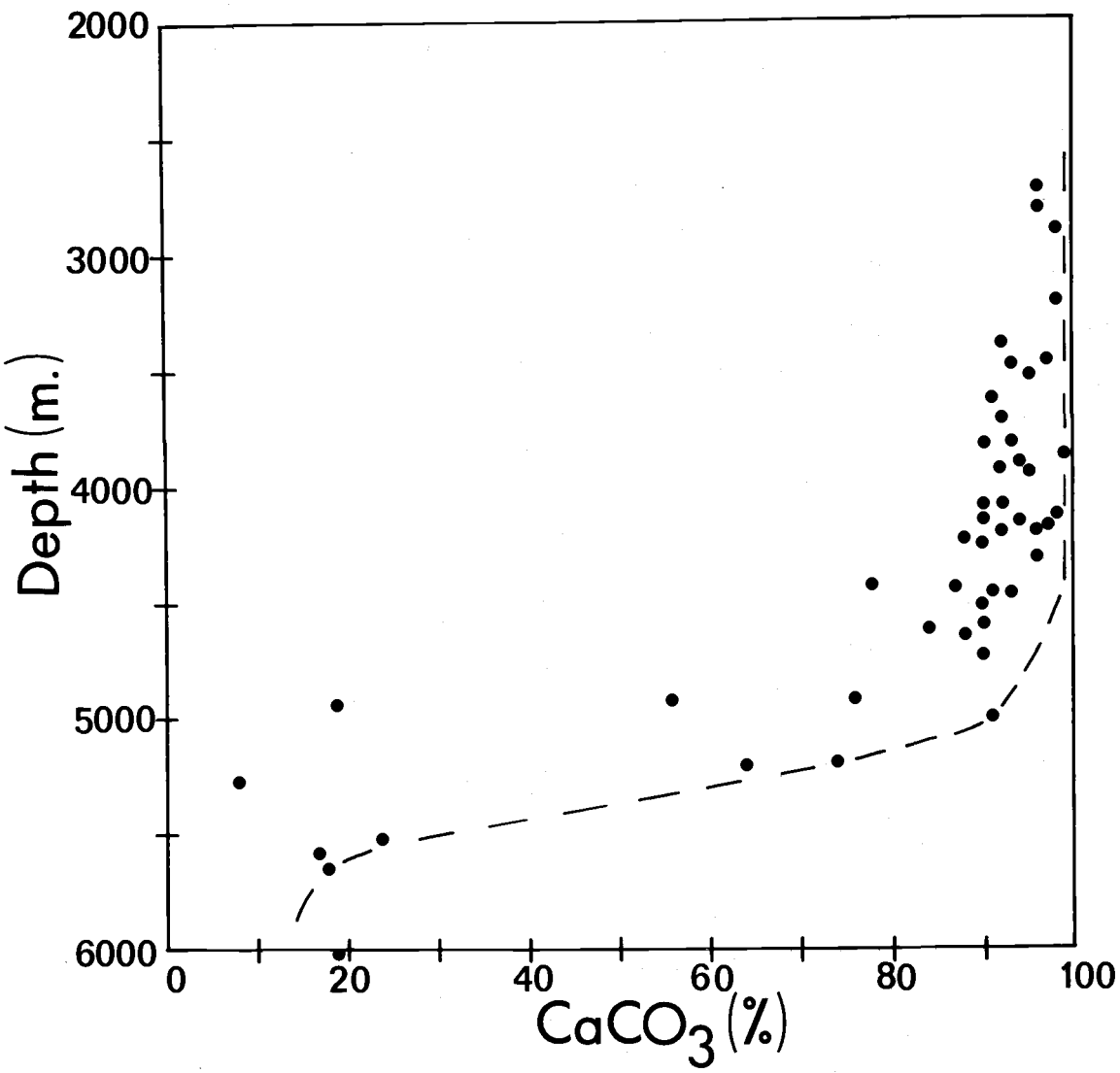

Figure 12. $CaCO_3$ vs. depth - Angola Basin.
The dashed line indicates the calcite compensation level.

for the compensation level.

The high percentage (more than half) of samples containing 90% $CaCO_3$ shows the uniform conditions prevailing throughout most of the Angola Basin. It is tempting to ascribe all of the low $CaCO_3$ values to clay dilution. However, Berger's (1968) report of the existence of a lysocline indicates that some carbonate dissolution is occurring.

Total South Atlantic

The three basins and their associated compensation levels are combined in Figure 13. It is apparent from these points that a single line for the compensation depth in the total South Atlantic Ocean cannot be determined. Only by separating the points by their respective basins can reasonable levels be established. Otherwise, the Angola Basin compensation level, being the deepest, would entirely control the line drawn.

Basin-wide averages are obtained by averaging all the carbonate values below 2000 m over 500 m depth intervals and assigning this average to the mid-point of the interval. Using the method of Heath and Culberson (1970) and assuming a constant non-carbonate dilutant of six percent for the Angola, Brazil and Argentine Basins and a dilutant of ten percent for the Cape Basin (dilutant percentages based upon the upper limit of $CaCO_3$ averages), the following values

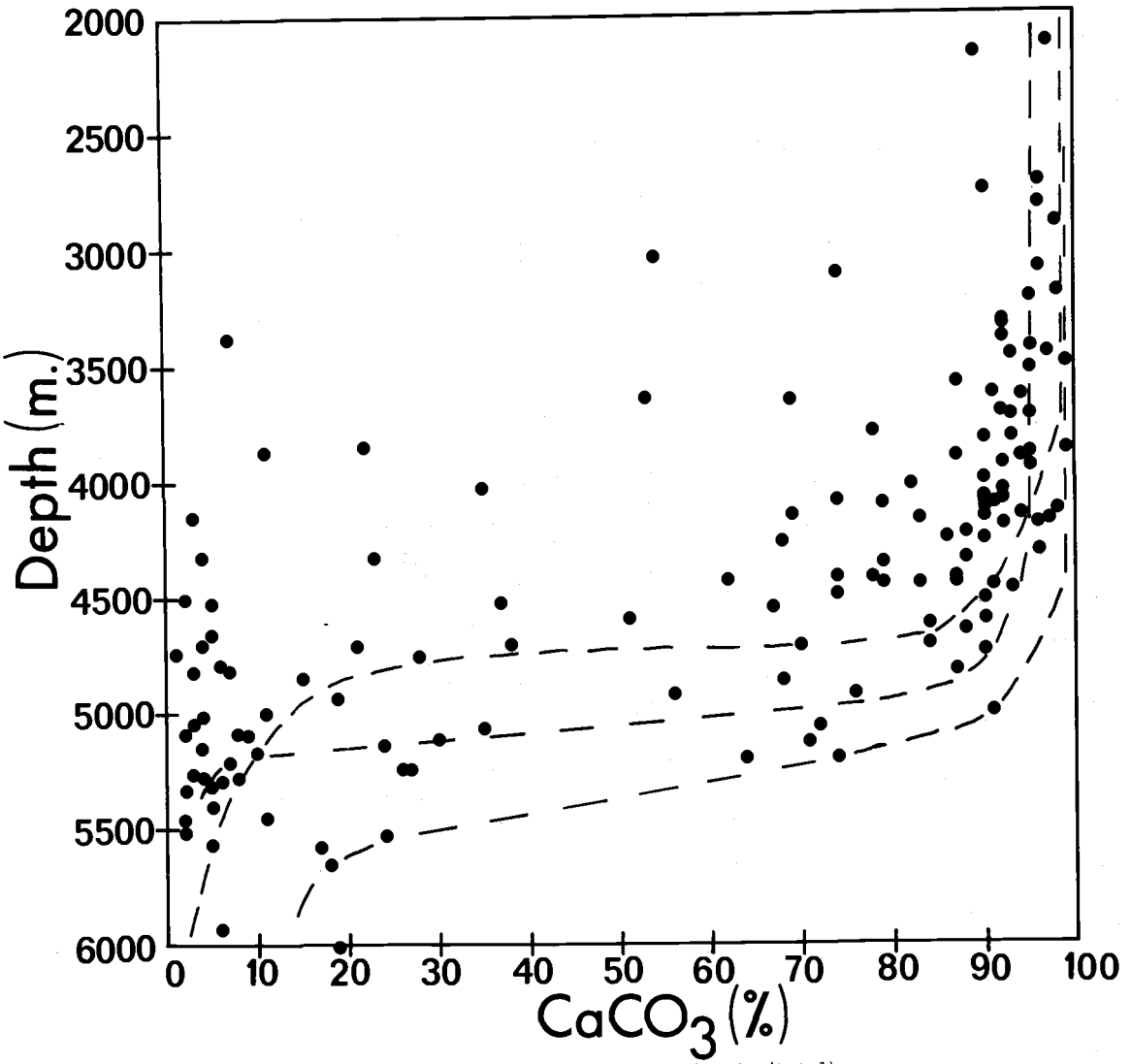

Figure 13. $CaCO_3$ vs. depth - South Atlantic (total). The dashed lines indicate the calcite compensation levels for all three basins. Top line: Brazil Basin; middle line: Cape Basin; bottom line: Angola Basin.

for the percentages of dissolution with depth result (Table 2).

The most striking feature of Table 2 is the great increase in dissolution percentages at relatively shallow depths. The Angola Basin depth of greatest increase (4500 m), although 1500 m deeper than those for the other basins, is still 1000 m above the compensation level and 700 m above Berger's (1968) value for the lysocline. In the other basins, the depth of greatest increase in solution (3000 m) is 1400 m above the lysocline and about 2000 m above the compensation level. By applying the assumptions of Heath and Culberson (1970) (constant rate of carbonate and of dilutant supply and solution only on the sea-floor) the changes in dissolution may be said to reflect changes in the rate of dissolution. The increase in dissolution at 3000 m is consistent with Berger's (1967) increase in rates of solution of foraminifera at 3000 m. However, the large discrepancy between the depth of greatest increase in solution (Heath and Culbersons (1970) interpretation of the lysocline) and Berger's (1968) values for the South Atlantic lysocline points out a weakness in its original definition. The level of the maximum rate of change of foraminiferal solution indices and the level at which the rate of dissolution of calcite increases abruptly are not always synonymous. A systematic weight decrease in foraminifera without complete dissolution of the less resistant species could produce the 700m-1400 disparity in the two levels.

The large compensation level differences between basins must

Table 2. Averages of Calcite Content and Percentage of Dissolution with Depth.

Depth (m)	Angola Basin		Brazil and Argentine Basins		Cape Basin	
	% $CaCO_3$	% Dissolution	% $CaCO_3$	% Dissolution	% $CaCO_3$	% Dissolution
2250	--	--	97	0	89	0
2750	97	0	--	0 (assumed)	90	0
3250	94	0	87	54	52*	79
3750	94	0	75	76	78	55
4250	91	33	67	82	78	55
4750	74	77	30	91	43	82
5250	59	85	9	93	36	84
5750	20	93	4	94	--	--

* Poor areal coverage

be considered in determining paleo-compensation depths, particularly in the South Atlantic. Otherwise, a sampling bias within an epoch could create an error on the order of 500 m. The factors controlling the present compensation level are considered in the following section.

Biological and Physico-Chemical Factors

The three most probable dominant controls on the compensation level are productivity, solution and dilution. Dilution has been mentioned above; productivity and solution will now be discussed in detail.

The assumption that surface productivity is directly related to $CaCO_3$ concentrations in sediments is implicit in several discussions, such as Bramlette (1961). Comparison of Meteor expedition data on surface productivity (Hentschel, 1933) with the data from this study permits a test of this assumption.

Hentschel (1933) constructed a map of the number of total planktonic organisms captured within the top 50 m of the water column. Steeman Nielsen and Jensen (1957) found a close correlation between the number of plankton present off the coast of southwestern Africa and the organic productivity from these organisms. By converting the Meteor values for standing crop to productivity in grams C/m^2, they obtained an extrapolated map of the entire South Atlantic identical to that of Hentschel (1933). The Hentschel contour map has

been used to obtain standing crop values.

In Figure 14 and 15, the percentages of $CaCO_3$ and carbonate-free opal are plotted versus their standing crop values. The standing crop values in Figures 14 and 15 represent the following contour intervals:

35	20-50	thousand plankton/liter
15	10-20	" "
7	5-10	" "
3	2- 5	" "
1	0- 2	" "

Since the opal and $CaCO_3$ values for any given standing crop do not represent a normal distribution, the medians have been used as the measure of central tendency. The shaded area indicates the 80% confidence limits.

There is no correlation between $CaCO_3$ content and productivity. The wide scatter in the data and between the 80% confidence limits precludes any meaningful relationship between the two variables.

The correlation between opal and productivity is somewhat better than that between $CaCO_3$ and productivity. As Figure 15 shows, there is a general increase in opal sediment content with increasing productivity levels. However, the significance of any opal-productivity correlation based on these data is due more to comparison of their mapped patterns and to the contrast with the

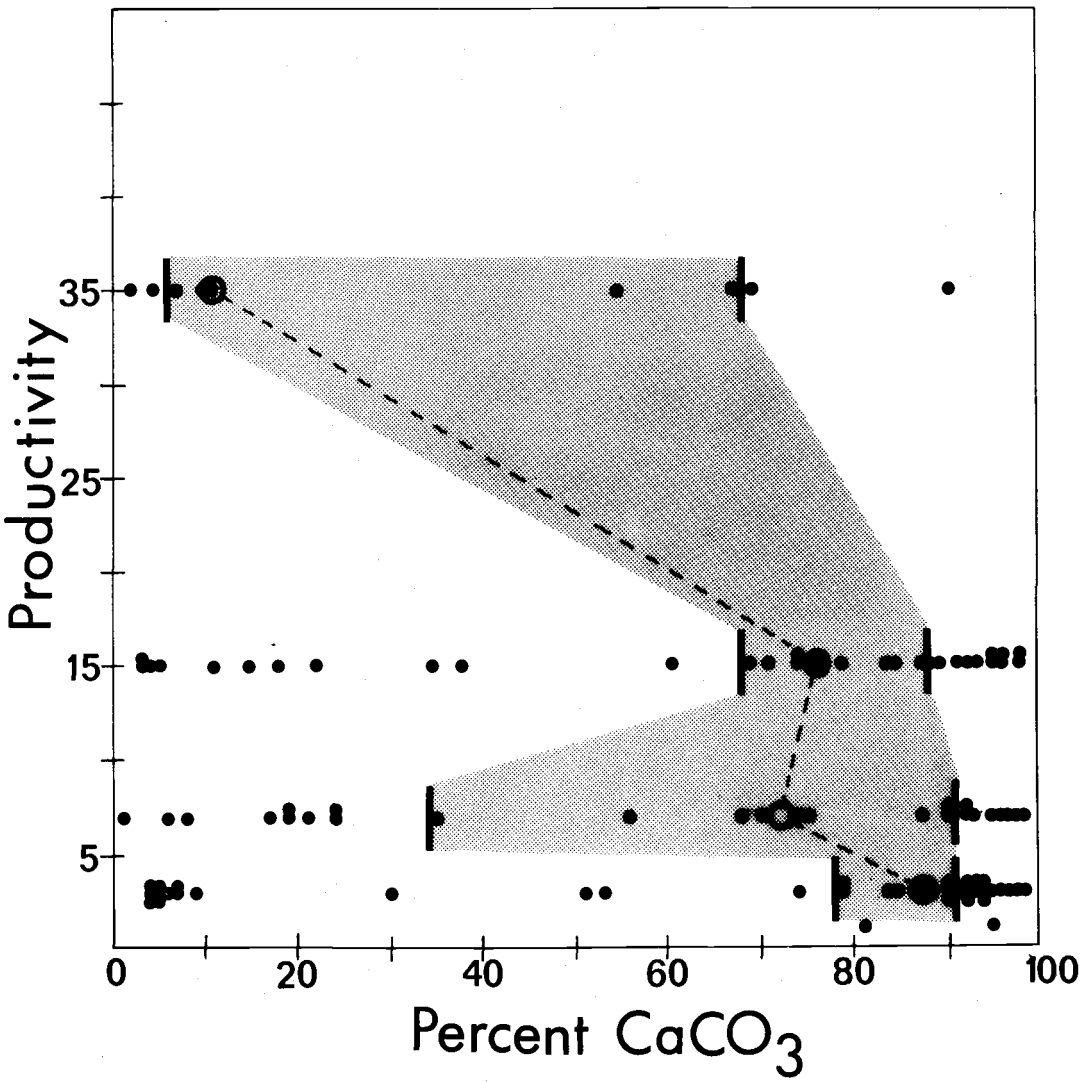

Figure 14. $CaCO_3$ vs. standing crop in thousands of plankton organisms in the upper 50 m. The medians are circled and connected with the dashed line. The area within the 80 percent confidence limits is shaded.

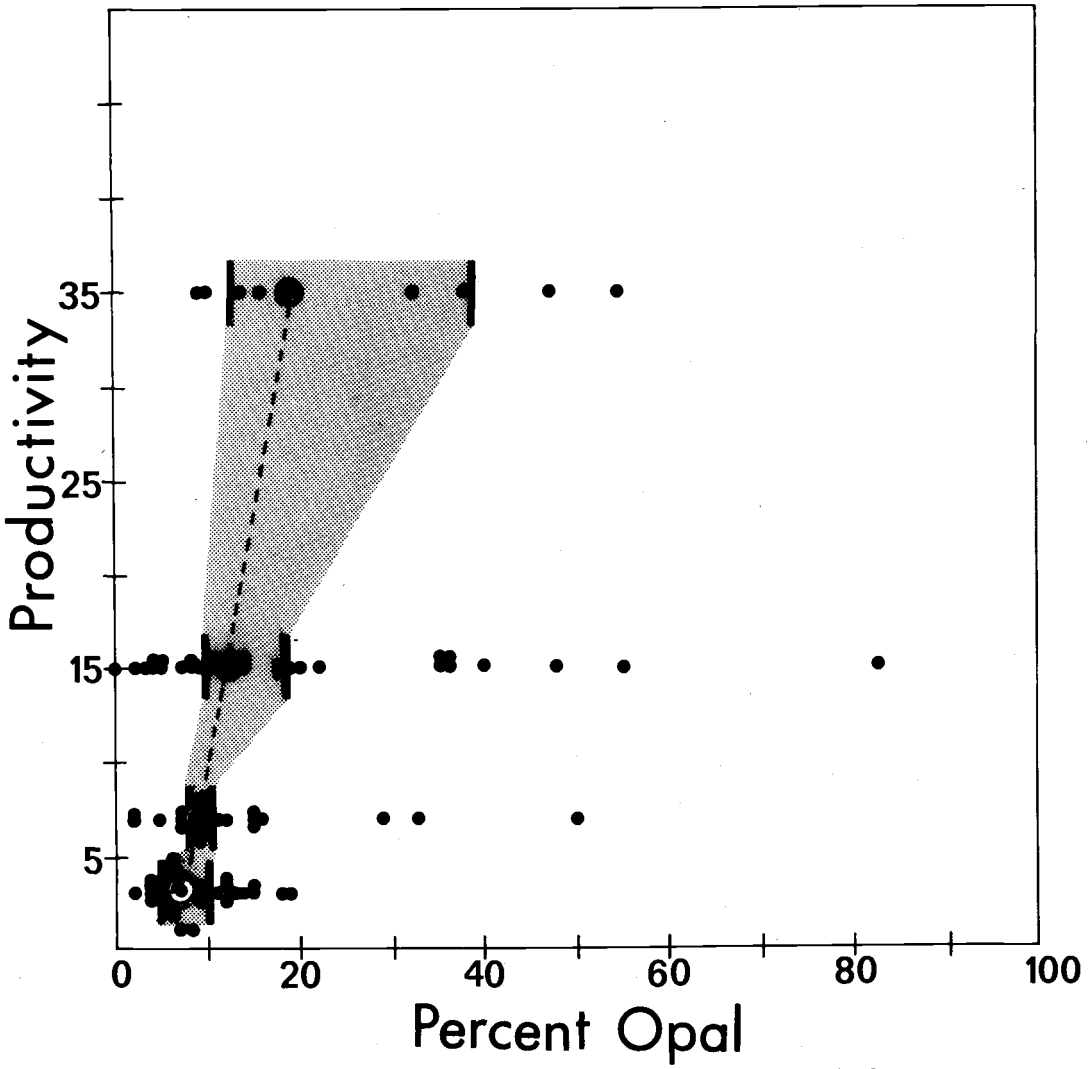

Figure 15. Opal vs. standing crop in thousands of plankton organisms in the upper 50 m. The medians are circled and connected with the dashed line. The area within the 80 percent confidence limits is shaded.

carbonate-productivity plot than to any intrinsic value of the correlation.

In order to evaluate the relation of calcite dissolution to bottom water masses, the water temperatures (quasi-conservative properties of water masses in the area under study) have been compared to the calcite contents of sediments at a number of stations.

Determinations of bottom water temperatures were made by consulting the Meteor Atlas (Wust and Defant, 1936) and the Atlantic Ocean Oceanographic Atlas (Fuglister, 1960). Cross-indexing of the depth and longitude permitted the location of those cores lying within one degree of the Atlantic cross-sections made at 8°, 16°, 21°, 24°, 27°-30°, 32°, 35°, 42° and 49° S. Isotherms along these sections are shown at intervals of 0.1° C. Therefore, in situ temperatures can be found for those samples which lie near a cross-section. A plot of the percentage calcium carbonate versus the isotherms is shown in Figure 16. Points representing Angola Basin samples are circled.

The figure shows a marked resemblance to a Bramlette-type compensation depth curve (Bramlette, 1961) with the level of compensation coinciding with the 1.1°-1.0° isotherms. This feature is not caused by selective sampling. A plot of depth versus the calcium carbonate percentage for the same samples does not show a well defined compensation level, but reflects the differences between the

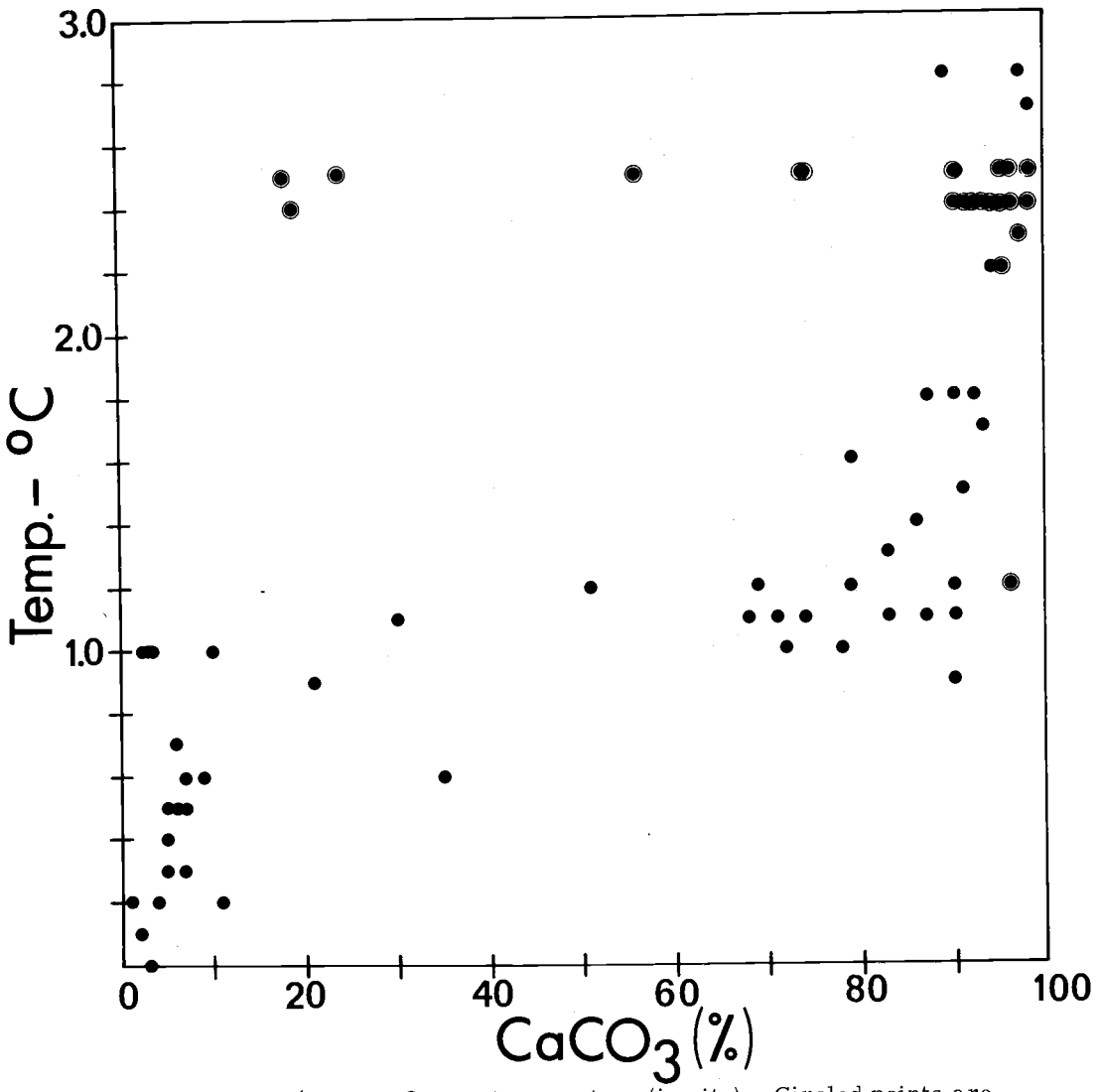

Figure 16. $CaCO_3$ vs. temperature (in situ). Circled points are Angola Basin samples.

various basins. These geographical differences, with the exception of some Angola Basin samples, are resolved by the isotherm plot. However, it should be noted that cold water and turbidity currents must follow similar paths, and therefore the low temperature points are also subject to possible turbidity current dilution.

The high-temperature, low-carbonate points are the deepest and easternmost of those Angola Basin samples plotted. This fact suggests that a high clay input from the Congo River resulting in dilution of the carbonate could account for the low calcium carbonate values.

A geographical comparison may be made between the 1° isotherm and the regions of steep contour gradients of the $CaCO_3$ percentages. The 1° isotherm (Wust, 1936) aligns well with the intermediate range $CaCO_3$ values along the west side of the Mid-Atlantic Ridge. Wust does not show isotherms in regions shallower than 4000 meters; therefore, the 1° isotherm is absent between its intersection with the Rio Grande Rise and the Cape Basin - Mid-Atlantic Ridge interface. An interpolation between the two endpoints results in a 1° isotherm which crosses the Mid-Atlantic Ridge at about 42° S. The shape of the isotherm is identical to the carbonate contours, but displaced slightly higher, or to the north of the 80% $CaCO_3$ contour. Within the Cape Basin, the correspondence is not quite so good. However, the main feature of the pattern - a tongue

of cold water which extends northward to the edge of the Walvis Ridge - is reflected by lower carbonate values in the same area. In most of the Cape Basin, the 1.2° isotherm correlates more closely with the areas of intermediate carbonate values than does the 1.0° isotherm.

It should be emphasized that the temperature values are important as quasi-conservative marker properties of the AABW, not as physico-chemical parameters of any great significance in the solution geochemistry of calcite. There is no evidence that the 0.3° C temperature change from 0.9° to 1.2° C changes the rate of solution of calcite any more than the same change in slightly warmer or cooler waters (MacIntyre, 1965).

SUMMARY

The South Atlantic Ocean has been chosen as the area for measurements of calcite, opal and quartz concentrations. The abundance of data and sediment samples in existence was the reason for its selection. A method for the quantitative determination of opal has been described. A clay parameter has been deduced from the difference between the sum of calcite, opal and quartz and 100 percent.

The South Atlantic is a carbonate ocean; calcite concentrations overshadow those of opal and quartz. Bottom water circulation and depth are the most important factors determining the distribution of calcite. Clay is next to calcite in importance in setting sedimentary patterns, and in the northeastern Angola Basin it is probably more important. Since the clay consists of terrigenously derived kaolinite and illite, it is likely a better indicator of continental input than quartz, which contains a significant ice-rafted component south of 35° S. Otherwise, quartz is high close to coasts, and low in the center of the ocean. Opal, which occurs in somewhat greater concentrations than quartz, is found in two bands across the north and south of the study area. This areal distribution resembles productivity patterns, particularly that of diatoms. Opal concentrations are positively correlated with surface productivity values.

The calcite compensation level is not easily determined for the South Atlantic as a whole; it is necessary to divide the data into basins. The compensation levels obtained are: Brazil and northern Argentine Basins - 4800 m; Cape Basin - 5100 m; Angola Basin - deeper than 5400 m. There is no correlation of calcium carbonate with surface productivity; while calcite concentrations decrease rapidly in in situ water temperatures of 1° C and less. Combined with the explanation of calcite patterns by bottom water circulation, these facts suggest that physico-chemical factors are more important than biological factors in setting the calcite compensation level.

BIBLIOGRAPHY

Arrhenius, G. O. S. 1963. Pelagic sediments. In: The Sea, ed. by M. N. Hill. Vol. 3. New York, Interscience. p. 655-727.

Be, A. W. H. and D. S. Tolderlund. 1971. Distribution and ecology of living planktonic foraminifera in surface waters of the Atlantic and Indian Oceans. In: The Micropaleontology of Oceans, ed. by B. M. Funnel and W. R. Riedel, Cambridge, 1971. Cambridge University Press. p. 105-149.

Berger, W. H. 1967. Foraminiferal ooze: solution at depths. Science. 156:383-385.

_____ 1968. Planktonic foraminifera: selective solution and paleoclimatic interpretation. Deep-Sea Research. 15:31-43.

_____ 1970. Planktonic foraminifera: selective solution and the lysocline. Marine Geology. 8:111-138.

Biscaye, P. E. 1965. Mineralogy and sedimentation of Recent deep-sea clay in the Atlantic Ocean and adjacent seas and oceans. Geol. Soc. Am. Bull. 76:803-832.

Biscaye, P. E. and E. J. Dasch. 1968. Source of Argentine Basin sediment, southwestern South Atlantic Ocean. Geol. Soc. Am. Abstracts. p. 28.

Bramlette, M. N. 1961. Pelagic sediments. In: Oceanography: Lectures at the International Oceanographic Congress, ed. by Mary Sears, New York, 1959. American Association for the Advancement of Science Publication 67. p. 345-366.

Broecker, W. S., K. K. Turekian and B. C. Heezen. 1958. The relation of deep-sea sedimentation rates to variations in climate. Am. J. Sci. 256:503-517.

Burckle, L. H. and P. E. Biscaye. 1971. Sediment transport by Antarctic Bottom Water through the eastern Rio Grande Rise. Geol. Soc. Am. Abstracts. 3:518-519.

Calvert, S. E. 1966. Accumulation of diatomaceous silica in the sediments of the Gulf of California. Geol. Soc. Am. Bull. 77:569-596.

Chester, R. and H. Elderfield. 1968. The infrared determination of opal in siliceous deep-sea sediments. Geochimica et Cosmochimica Acta. 32:1128-1140.

Dasch, E. Julius, F. A. Hills and K. K. Turekian. 1966. Strontium isotopes in deep-sea sediments. Science. 153:295-297.

Edmond, John M. 1970. The carbonic acid system in sea water. Ph. D. Thesis. San Diego, University of California. 174 numb. leaves.

Ewing, M., X. Le Pichon and J. Ewing. 1966. Crustal structure of the mid-ocean ridges, 4, sediment distribution in the South Atlantic Ocean and the Cenozoic history of the Mid-Atlantic Ridge. J. Geophys. Res. 71:1611-1636.

Fuglister, F. C. 1960. Atlantic Ocean Atlas. Woods Hole, Massachusetts, Woods Hole Oceanographic Institution. 209 p.

Goldberg, E. D. 1958. Determination of opal in marine sediments. J. Mar. Res. 17:178-182.

_____ 1968. Ionium/thorium geochronologies. Earth and Planetary Science Letters. 4:17-21.

Goldberg, E. D. and J. J. Griffin. 1964. Sedimentation rates and mineralogy in the South Atlantic. J. Geophys. Res. 69:4293-4309.

Goldberg, E. D. and Minoru Koide. 1962. Geochronological studies of deep-sea sediments by the ionium/thorium method. Geochimica et Cosmochimica Acta. 26:417-450.

Hashimoto, I. and M. L. Jackson. 1960. Rapid dissolution of allophane and kaolinite-halloysite after dehydration. In: Proceedings of the Seventh National Conference on Clays and Clay Minerals, Washington, D. C., 1958. Pergamon. p. 102-113.

Heath, G. R. and C. Culberson. 1970. Calcite: degree of saturation, rate of dissolution and the compensation depth in the deep oceans. Geol. Soc. Am. Bull. 81:3157-3160.

Heezen, B. C. et al. 1964. Congo submarine canyon. Bull. of A. A. P. G. 48:1126-1149.

Hentschel, E. 1933. Allgemeine biologie des Sudatlantischen Ozeans. Dt. Atlant. Exped. Meteor, 1925-1927. 11:1-168.

Hollister, C. D. and R. B. Elder. 1969. Contour currents in the Weddell Sea. Deep-Sea Res. 16:99-101.

Jones, E. L. W., M. Ewing, J. I. Ewing and S. L. Eittrem. 1970. Influence of Norwegian Sea overflow water on sedimentation in the northern North Atlantic and Labrador Sea. J. Geophys. Res. 75:1655-1680.

Kennett, J. P. 1966. Foraminiferal evidence of a shallow calcium carbonate solution boundary, Ross Sea, Antarctica. Science. 153:191-193.

Ku, T. L., W. S. Broecker and Neil Opdyke. 1968. Comparison of sedimentation rates measured by paleomagnetic and the ionium methods of age determination. Earth and Planetary Science Letters. 4:1-16.

Lisitzin, A. P. 1971. Distribution of siliceous microfossils in suspension and in bottom sediments. In: The Micropaleontology of Oceans, ed. by M. N. Funnel and W. R. Riedel, Cambridge, 1971. Cambridge University Press. p. 173-195.

MacIntyre, W. G. 1965. The temperature variation of the solubility product of calcium carbonate in seawater. Fish Res. Bd. of Canada, Manuscript Rep. Ser. 200, Ottawa, Canada. 153 p.

Maxwell, Arthur E. et al. 1970. Deep Sea drilling in the South Atlantic. Science. 168:1047-1059.

Murray, J. and A. F. Renard. 1891. Deep-sea deposits based on the specimens collected during the voyage of H. M. S. Challenger in the years 1872 to 1876. Report of the Voyage of the Challenger. London, Longmans. 525 p.

Olsen, Boyd. E. 1968. On the abyssal temperatures of the world oceans. Ph. D. Thesis. Corvallis, Oregon State University. 151 numb. leaves.

Peterson, M. N. A. 1966. Calcite: rates of dissolution in a vertical profile in the central Pacific. Science. 154:1542-1544.

Pratje, Otto. 1939. Sediments of South Atlantic Ocean. Bull. Am. Assoc. Pet. Geol. 23:1666-1672.

Smith, R. L. 1968. Upwelling. Oceanogr, Mar. Biol, Ann. Rev. 6:11-46.

Steeman Nielsen, E. and E. Aabye Jensen. 1957. Primary oceanic production. The autotrophic production of organic matter in the oceans. Galathea Rep. 1:49-120.

Till, R. and D. A. Spears. 1969. The determination of quartz in sedimentary rocks using an X-ray diffraction method. Clays and Clay Minerals. 17:323-327.

Turekian, K. K. 1964. The geochemistry of the Atlantic Ocean basin. Transactions of the New York Academy of Sciences. 26:312-330.

Turekian, K. K. and Minze Stuiver. 1964. Clay and carbonate accumulation rates in three South Atlantic deep-sea cores. Science. 146:55-56.

Wust, G. 1936. Das Bodenwasser und die Gliederung der Atlantischen Tiefsee. Dt. Atlant. Exped. Meteor 1925-1927. 6:1-106.

Wust, G. and A. Defant. 1936. Schichtung und Zirkulation des Atlantischen Ozeans. Dt. Atlant. Exped. Meteor 1925-1927. 6:Atlas.

APPENDICES

APPENDIX I. Sample Locations

Sample	Latitude (°S)	Longitude	Water Depth (m)	Sample Interval
Chain 99 Cores:				
3-15	4° 35'	19° 02' W	4349	Top
3-16	6° 38'	18° 55' W	4713	Top
3-24A	7° 20'	14° 05' W	3722	Top
3-26	8° 23'	13° 04' W	3116	Top
3-29	8° 39'	9° 27' W	3714	Top
3-37	8° 39'	2° 05' E	5658	Top
Circe Cores:				
143 P	25° 40'	7° 10' E	4106	5-7
144 G	25° 46'	9° 26' E	4554	3-6
216 G	8° 04'	5° 29' E	4942	0-5
220 P	7° 34'	1° 32' W	4313	2-5
227 P	7° 49'	6° 14' W	4178	4-6
240 F	8° 17'	11° 07' W	3201	3-5
Lusiad Cores:				
LSDA 159	33° 51'	15° 07' E	4150	0-4
LSDA 163	31° 21'	1° 58' E	4190	0-3
LSDA 167	29° 42'	7° 20' W	4152	0-5
LSDA 168	28° 51'	9° 25' W	3930	8-12

APPENDIX I (Continued)

Sample	Latitude (°S)	Longitude	Water Depth (m)	Sample Interval
LSDA 178	24° 03'	15° 32' W	4045	0-5
LSDA 183	19° 44'	12° 55' W	3500	0-5
LSDA 185	18° 33'	10° 17' W	3460	5-7
LSDA 199G	5° 42'	11° 14' W	2900	4-6
Vema Cores:				
9- 11	3° 13'	32° 12' W	4715	0-2
9- 16	8° 25'	22° 29' W	5937	Top
9- 18	8° 59'	15° 55' W	4005	10
9- 22	8° 09'	18° 38' W	4735	10
12- 16	26° 20'	29° 28' W	5570	0-2
12- 18	28° 42'	34° 30' W	4022	5-7
12- 52	39° 36'	32° 52' W	5016	8-10
12- 53	40° 54'	20° 23' W	3797	0-10
12- 54	41° 14'	6° 07' W	4082	0-10
12- 66	22° 59'	7° 01' E	2759	1-4
12- 73	5° 54'	9° 53' E	3054	0-3
16- 32	13° 54'	22° 47' W	5276	10
16- 33	15° 20'	19° 43' W	4360	Top
16- 34	17° 02'	16° 13' W	3530	8-9

APPENDIX I (Continued)

Sample	Latitude (°S)	Longitude	Water Depth (m)	Sample Interval
16- 36	19° 22'	11° 26' W	3329	4-7
16- 37	21° 20'	8° 57' W	3908	0-3
16- 38	22° 59'	6° 46' W	4925	7
16- 39	24° 44'	4° 46' W	4596	3-6
16- 44	30° 58'	5° 26' E	5127	5
16-186	32° 55'	40° 25' W	4746	5
16-187	31° 28'	40° 05' W	3643	9-10
18-163	36° 58'	37° 47' W	5000	3-7
18-164	36° 34'	34° 02' W	4525	10
18-165	36° 10'	30° 02' W	4328	Top
18-166	34° 29'	27° 07' W	4527	5-8
18-167	33° 29'	23° 41' W	4265	9-10
18-169	30° 30'	16° 16' W	3319	Top
18-173	30° 23'	9° 26' W	3815	0-1
18-174	30° 28'	6° 28' W	4651	5-7
18-175	31° 07'	3° 35' W	4146	Top
18-176	31° 11'	00° 54' E	4468	Top
18-180	33° 01'	8° 56' E	5050	4-8
19-241	29° 37'	10° 36' E	4493	4-6
19-244	27° 15'	6° 12' E	4865	0-2

APPENDIX I (Continued)

Sample	Latitude (°S)	Longitude	Water Depth (m)	Sample Interval
19-245	26° 12'	4° 42' E	2725	0-5
19-247	25° 25'	3° 20' E	5002	3-4
19-262	18° 20'	8° 23' E	4918	3-5
19-263	16° 55'	6° 36' E	5278	Top
19-267	13° 23'	2° 13' E	5585	Top
20-209	28° 26'	7° 45' W	4257	Top
20-212	28° 13'	10° 02' W	3523	0-2
20-215	28° 38'	16° 21' W	4114	Top
20-216	28° 41'	18° 50' W	4451	Top
20-217	28° 33'	23° 03' W	4601	Top
20-218	28° 40'	27° 38' W	5115	0-8
20-219	29° 02'	29° 13' W	3092	6-8
20-221	22° 53'	28° 53' W	5298	8-9
20-222	19° 29'	28° 07' W	5148	Top
20-223	15° 21'	28° 44' W	5318	Top
20-224	13° 00'	30° 10' W	5405	Top
20-225	9° 48'	31° 19' W	5214	Top
20-226	7° 38'	32° 05' W	5092	Top
22-101B	49° 09'	26° 00' W	4506	Top
22-103	49° 50'	21° 24' W	3871	3-6

APPENDIX I (Continued)

Sample	Latitude (°S)	Longitude	Water Depth (m)	Sample Interval
22-104	49° 00'	19° 29' W	4321	5
22-106	46° 08'	10° 54' W	3037	7
22-107	44° 28'	6° 38' W	3898	0-3
22-108	43° 11'	3° 15' W	4171	8-9
22-109	41° 58'	00° 15' W	733	8-10
22-110	39° 45'	5° 06' E	5145	10
22-113	37° 33'	9° 56' E	5073	10
22-115	36° 01'	13° 41' E	4854	10
22-139	35° 05'	8° 22' E	4825	8-9
22-140	33° 37'	2° 21' E	4433	10
22-146	32° 21'	2° 10' E	2177	0-1
22-159	28° 43'	1° 55' E	3471	Top
22-163	26° 22'	00° 56' E	4442	Top
22-165	23° 08'	00° 31' E	5198	10
22-166	20° 38'	1° 57' W	5530	0-5
22-167	18° 43'	3° 54' W	6020	4-7
22-168	17° 18'	5° 11' W	4625	Top
22-170	14° 38'	7° 34' W	4131	1-3
22-173	12° 23'	10° 09' W	3878	0-2
24-219	34° 51'	4° 09' E	5174	4-6

APPENDIX I (Continued)

Sample	Latitude (°S)	Longitude	Water Depth (m)	Sample Interval
24-222	34° 13'	3° 12' W	3944	0-2
24-225	34° 54'	4° 57' W	1790	7-8
24-228	34° 55'	7° 48' W	4085	0-2
24-229	34° 27'	10° 36' W	4202	5-6
24-231	33° 57'	13° 50' W	3438	0-2
24-235	33° 15'	19° 33' W	3722	0-2
24-238	31° 47'	29° 00' W	3585	2
24-242	31° 32'	30° 57' W	4089	2
24-248	30° 39'	36° 59' W	2131	0-2
24-250	30° 11'	39° 22' W	4813	3-5
24-254	22° 58'	36° 43' W	4029	0-3
Conrad Cores:				
8-15	19° 20'	20° 32' W	4707	10-11
8-16	23° 21'	16° 32' W	4440	10-11
8-19	24° 18'	14° 42' W	3636	4-6
8-28	26° 34'	9° 26' W	4089	9-10
11-79	49° 00'	4° 36' W	3385	0-2
11-80	46° 45'	00° 03' W	3656	3-5
11-81	43° 54'	5° 13' E	4704	3-5
11-83	41° 36'	9° 43' E	4718	Top

APPENDIX II. Concentrations of $CaCO_3$, Opal, Quartz and "Clay"

Sample	$CaCO_3$	Opal	Qtz.	Opal % of Total	Qtz. % of Total	"Clay"
CH3-15	88	35	9	4	1	7
CH3-16	84	22	10	4	2	10
CH3-24	95	35	6	2	0	3
CH3-26	74	40	5	10	1	15
CH3-29	92	57	8	5	1	2
CH3-37	18	12	13	10	11	61
C1R143	79	9	12	2	3	16
C1R144	67	14	11	5	4	24
C1R216	19	33	6	27	5	49
C1R220	96	29	5	1	0	3
C1R227	97	50	9	2	0	1
C1R240	98	47	6	1	0	1
LSDA159	69	11	34	3	11	17
LSDA163	96	19	11	1	0	3
LSDA167	94	12	11	1	1	4
LSDA168	92	11	12	1	1	6
LSDA178	92	13	10	1	1	6
LSDA183	99	12	6	0	0	1

APPENDIX II (Continued)

Sample	$CaCO_3$	Opal	Qtz.	Opal % of Total	Qtz. % of Total	"Clay"
LSDA185	97	11	5	0	0	3
LSDA199	98	83	5	2	0	0
V 9-11	70	5	10	2	3	25
V 9-16	6	8	8	8	8	78
V 9-18	90	14	3	1	0	9
V 9-22	90	27	12	3	1	6
V12-16	5*	8	7	8	7	80
V12-18	82	7	13	1	2	15
V12-52	4	10	19	10	18	68
V12-53	78	14	13	3	3	16
V12-54	90	9	4	1	0	9
V12-66	90	16	12	2	1	7
V12-73	4*	11	11	9	9	78
V16-32	4	6	12	6	12	78
V16-33	79	12	8	3	2	16
V16-34	95	4	4	0	0	5

* Value from K. K. Turekian; V12-73 omitted from plots.

APPENDIX II (Continued)

Sample	$CaCO_3$	Opal	Qtz.	Opal % of Total	Qtz. % of Total	"Clay"
V16-36	92	5	8	0	1	7
V16-37	94	4	9	0	1	5
V16-38	56	10	11	4	5	35
V16-39	90	6	9	1	1	8
V16-44	71	3	7	1	2	26
V16-186	1	8	15	8	15	76
V16-187	53	6	16	3	8	36
V18-163	11	14	15	12	13	64
V18-164	5	8	43	8	41	46
V18-165	23	10	55	8	42	27
V18-166	37	9	15	6	9	48
V18-167	68	0	2	0	1	31
V18-169	92	SPILLED				
V18-173	93	9	10	1	1	5
V18-174	88	7	12	1	1	10
V18-175	90	15	11	2	1	7
V18-176	93	4	6	0	0	7
V18-180	3	4	10	4	10	83

APPENDIX II (Continued)

Sample	$CaCO_3$	Opal	Qtz.	Opal % of Total	Qtz. % of Total	"Clay"
V19-241	74	2	0	1	0	25
V19-244	68	15	12	5	4	23
V19-245	96	3	9	0	0	4
V19-247	91	8	10	1	1	7
V19-262	76	0	2	0	0	24
V19-263	8	2	14	2	13	77
V19-267	17	15	12	13	10	60
V20-209	90	15	13	2	1	7
V20-212	95	8	8	0	0	5
V20-215	91	9	10	1	1	7
V20-216	83	7	9	1	2	14
V20-217	51	2	2	1	1	47
V20-218	30	7	14	5	10	55
V20-219	96	6	12	0	0	4
V20-221	6	6	13	6	12	76
V20-222	4	6	12	6	12	78
V20-223	5	6	13	6	12	77
V20-224	5	6	13	6	12	77
V20-225	7	4	13	4	12	77

APPENDIX II (Continued)

Sample	$CaCO_3$	Opal	Qtz.	Opal % of Total	Qtz. % of Total	"Clay"
V20-226	9	6	17	5	15	71
V22-101	2	10	16	10	16	72
V22-103	11	38	11	34	11	44
V22-104	4	46	15	44	14	38
V22-106	54	32	18	15	9	22
V22-107	87	36	8	5	1	7
V22-108	83	36	7	6	1	10
V22-109	98	9	2	0	0	2
V22-110	24	17	14	13	11	52
V22-113	35	20	31	13	20	32
V22-115	15	7	63	6	54	24
V22-139	3	11	2	11	2	84
V22-140	62	12	13	5	5	28
V22-146	89	5	0	1	0	10
V22-159	93	18	11	1	1	5
V22-163	87	15	11	2	1	10
V22-165	74	5	10	1	3	22
V22-166	24	7	18	5	14	57
V22-167	19	11	10	9	8	64

APPENDIX II (Continued)

Sample	$CaCO_3$	Opal	Qtz.	Opal % of Total	Qtz. % of Total	"Clay"
V22-168	84	19	8	3	1	12
V22-170	98	15	5	0	0	2
V22-173	99	7	4	0	0	1
V24-219	10	9	16	8	14	68
V24-222	95	14	6	1	0	4
V24-225	75	9	3	2	1	22
V24-228	92	9	5	1	0	7
V24-229	92	9	7	1	1	6
V24-231	95	8	7	0	0	5
V24-235	93	9	10	1	1	5
V24-238	87	8	11	1	1	11
V24-242	74	9	12	2	3	21
V24-248	97	12	8	0	0	3
V24-250	7	7	20	7	19	67
V24-254	35	7	32	5	21	39
RC8-15	4	4	7	4	7	85
RC8-16	79	10	12	2	3	16
RC8-19	94	8	9	0	1	5

APPENDIX II (Continued)

Sample	$CaCO_3$	Opal	Qtz.	Opal % of Total	Qtz. % of Total	"Clay"
RC8-28	90	14	13	1	1	8
RC11-79	7	19	13	18	12	63
RC11-80	69	55	9	17	3	11
RC11-81	38	18	22	11	14	37
RC11-83	21	9	20	7	16	56

APPENDIX III. Data used from K. K. Turekian

Sample	Latitude (°S)	Longitude	Water Depth (m)	$CaCO_3$
V12- 12	16° 34'	28° 02' W	5329	2
V12- 13	18° 52'	28° 37' W	5088	2
V12- 15	24° 41'	29° 17' W	5471	2
V12- 17	27° 29'	31° 58' W	4762	28
V12- 20	31° 09'	39° 28' W	4663	5
V12- 21	32° 22'	42° 01' W	3851	22
V12- 22	33° 43'	45° 17' W	4152	3
V12- 56	36° 30'	8° 06' E	3222	95
V12- 61	28° 28'	8° 42' E	5064	72
V12- 65	22° 59'	8° 06' E	4118	90
V12- 67	22° 56'	4° 53' E	2812	96
V12- 77	4° 48'	2° 45' E	5205	64
V12- 78	4° 23'	0° 11' W	4232	88
V12- 79	1° 31'	11° 47' W	3823	90
V16- 27	9° 05'	32° 57' W	4797	6
V16- 28	10° 35'	31° 02' W	5264	3
V16- 29	11° 06'	29° 15' W	5456	11
V16- 30	11° 44'	27° 37' W	5513	2
V16- 31	13° 04'	24° 41' W	4425	87

APPENDIX III (Continued)

Sample	Latitude (°S)	Longitude	Water Depth (m)	$CaCO_3$
V16- 35	17° 40'	15° 06' W	3891	95
V16- 40	26° 16'	3° 01' W	4740	90
V16- 41	27° 52'	1° 06' W	4463	91
V16- 42	29° 06'	0° 20' E	4511	90
V16- 43	30° 10'	3° 11' E	1006	96
V16- 46	32° 08'	10° 45' E	4821	87
V17-151	5° 23'	21° 26' W	5245	27
V17-152	3° 09'	19° 23' W	5245	26
V17-153	1° 34'	19° 13' W	4425	74
V18-162	38° 03'	42° 44' W	5088	8
V18-168	32° 10'	20° 10' W	4251	86
V18-171	30° 29'	12° 59' W	3389	92
V18-172	30° 25'	10° 29' W	3623	91
V18-177	31° 28'	0° 05' E	4425	78

All of the Turekian samples are core-tops.